Computational Fluid Dynamics Analysis of the Effects of Windshield Angle on Fuel Economy and Optimization for the Locally Assembled Anbessa Intercity Bus

Abreham Chala Debela

A Thesis submitted to the Department of Mechanical Engineering

School of Mechanical, Chemical and Materials Engineering

Presented in Partial Fulfillment of the Requirements for the Degree of Master's in Automotive Engineering.

Office of Graduate Studies

Adama Science and Technology University

June 2024

Adama, Ethiopia

Computational Fluid Dynamics Analysis of the Effects of Windshield Angle on Fuel Economy and Optimization for the Locally Assembled Anbessa Intercity Bus

Abreham Chala Debela

Advisor: Alemayehu Wakjira (PhD)

A Thesis submitted to the Department of Mechanical Engineering

School of Mechanical, Chemical and Materials Engineering.

Presented in Partial Fulfillment of the Requirements for the Degree of Master's in Automotive Engineering.

Office of Graduate Studies

Adama Science and Technology University

June 2024

Adama, Ethiopia

DECLARATION

I hereby declare that this Master Thesis entitled "***Computational Fluid Dynamics Analysis of the Effects of Windshield Angle on Fuel Economy and Optimization for the Locally Assembled Anbessa Intercity Bus***" is my original work. That is, it has not been submitted for the award of any academic degree, diploma, or certificate in any other university. All sources of materials that are used for this thesis have been duly acknowledged through citation.

Abreham Chala Debela	______________________	June 2024
Name of the student	Signature	Date

RECOMMENDATION

I/we, the advisor(s) of this thesis, hereby certify that I/we have read the revised version of the thesis entitled "***Computational Fluid Dynamics Analysis of the Effects of Windshield Angle on Fuel Economy and Optimization for the Locally Assembled Anbessa Intercity Bus***" prepared under my/our guidance by **Abreham Chala Debela** submitted in partial fulfillment of the requirements for the degree of Mater's of Science in **Automotive Engineering**. Therefore, I/we recommend the submission of revised version of the thesis to the department following the applicable procedures.

______________________	______________________	______________
Major Advisor	Signature	Date
______________________	______________________	______________
Co-advisor	Signature	Date

APPROVAL

I/we, the advisors of the thesis entitled "***Computational Fluid Dynamics Analysis of the Effects of Windshield Angle on Fuel Economy and Optimization for the Locally Assembled Anbessa Intercity Bus***" and developed by Abreham Chala Debela hereby certify that the recommendation and suggestions made by the board of examiners are appropriately incorporated into the final version of the thesis.

___________________________	________________________	________________
Major Advisor	Signature	Date
___________________________	________________________	________________
Co-advisor	Signature	Date

We, the undersigned, members of the Board of Examiners of the thesis by **Abreham Chala Debela** have read and evaluated the thesis entitled "***Computational Fluid Dynamics Analysis of the Effects of Windshield Angle on Fuel Economy and Optimization for the Locally Assembled Anbessa Intercity Bus***" and examined the candidate during open defense. This is, therefore, to certify that the thesis is accepted for partial fulfillment of the requirement of the degree of Master of Science in Automotive Engineering.

________________________________	_____________________	________________________
Chairperson	Signature	Date
________________________________	_____________________	________________________
Internal Examiner	Signature	Date
________________________________	_____________________	________________________
External Examiner	Signature	Date

Finally, approval and acceptance of the thesis is contingent upon submission of its final copy to the Office of Postgraduate Studies (OPGS) through the Department Graduate Council (DGC) and School Graduate Committee (SGC).

Department Head	Signature	Date
School Dean	Signature	Date
Office of Postgraduate Studies, Dean	Signature	Date

ACKNOWLEDGEMENT

I would like to express my gratitude to the almighty God for giving me time, strength and health during the preparation of this thesis. My deepest gratitude goes to my Advisor, **Alemayehu Wakjira (PhD)**, for his help, advice and guidance that gave me direction and made me put intelligent effort on this thesis work. My special thanks go to my family and my friends, for their unwavering support and encouragement throughout my thesis. Then, I would like to express my sincere gratitude and appreciation to my classmates.

TABLE OF CONTENTS

LIST OF TABLES

LIST OF FIGURES

ACRONYMS AND ABBREVIATIONS

3D	-	*Three dimensional*
A	-	*Frontal area of the vehicle*
A_f	-	*Frontal area*
ACC	-	*Automatic Cruise Control*
ACBSE	-	*Anbassa City Bus Service Enterprise*
ANSYS	-	*Analysis System*
AVL	-	*Automatic Vehicle Location*
CD	-	*Coefficient of Drag*
C_D	-	*Drag coefficient*
C_L	-	*Lift coefficient*
CFD	-	*Computational Fluid Dynamics*
CVT	-	*Continuously Variable Transmissions*
DCT	-	*Dual-Clutch Transmissions*
E	-	*Energy consumption per Km-hour*
F_C	-	*Fuel consumption*
F_D	-	*Drag force*
F_L	-	*Lift force*
g	-	*Gravitational acceleration vector*
k	-	*Turbulent kinetic energy*
LES	-	*Large eddy simulation*
NREL	-	*National Renewable Energy Laboratory*
P	-	*Power required to overcome the drag, Pressure*
RANS	-	*Reynolds-averaged Navier-Stokes*
SST	-	*Shear Stress Transfer*
t	-	*Time*
u	-	*Velocity vector in x direction*
U	-	*Velocity vector*

v	-	*Air velocity, Velocity vector in y direction*
V_{Bus}	-	*Velocity of the vehicle*
w	-	*Velocity vector in z direction*
∇	-	*Gradient operator*
ε	-	*Turbulent kinetic energy dissipation rate*
μ	-	*Dynamic viscosity*
ρ	-	*Density of the fluid*
τ	-	*Shear Stress*
ω	-	*Turbulent kinetic energy specific dissipation rate*
ϕ_d	-	*Specific energy of the fuel*

ABSTRACT

Anbessa intercity bus has very poor external body shape, and hence has very high aerodynamic drag that significantly increases its fuel consumption. Various works have been done to improve fuel economy through reduction of drag coefficients using optimized windshields. Though, still, various city buses have suboptimal aerodynamic design, primarily owing to their vertical rectangular windshield configuration. And, this suboptimal design results in high aerodynamic drag, significantly increasing fuel consumption. One of such city buses is Anbessa city bus. However, by reducing the windshield angle, the drag force can be minimized, resulting in improved fuel economy. Thus, this compares six bus models with varying windshield angles, ranging from 19° to 45° using the Phoenics software. It is found that as the windshield angle increases, the drag coefficient decreases, leading to improved fuel efficiency. Specifically, the model with the lowest windshield angle of 19° exhibits the highest drag coefficient and the lowest fuel economy, while the optimized model of the bus which has highest windshield angle of 38.068^{O}, has the lowest drag coefficient and highest fuel economy. Furthermore, the optimization is performed using DESIGN EXPERT software to obtain the optimized model with desirability factor of 0.886 is to give a windshield angle of 38.068^{O} at which drag coefficient, lift coefficient, and fuel economy are 0.53, -0.07, and 5.967 respectively. While determining these values the calculation for drag coefficient, lift coefficient, and fuel economy obtains the R^2 value of 0.8727, 0.9375, and 0.9999, respectively. Thus, by increasing the windshield angle by 19.1^{O}, the fuel economy can be improved by 32.6%.

Keywords: *Aerodynamics, Drag, Fuel economy, Windshield Angle*

CHAPTER ONE

1. INTRODUCTION

1.1. Background of the Study

Fuel economy is of utmost importance in the automotive industry (Bechtold & Regency, 2018). It directly affects the operational costs of vehicles, particularly in sectors reliant on transportation, such as logistics and public transportation (Hicks, 2014). Improved fuel efficiency translates to reduced fuel consumption, leading to significant cost savings for vehicle owners and operators (Bechtold & Regency, 2018). Moreover, as fuel prices fluctuate and environmental concerns grow, achieving optimal fuel economy becomes crucial for both economical and sustainable reasons. By using more efficient engines, lightweight materials, aerodynamic designs, and developing new technologies, automotive industry is constantly working to improve fuel economy (Bayindirli & Celik, 2022).

Fuel economy and vehicle performance are closely linked (Bechtold & Regency, 2018). Optimal fuel efficiency allows vehicles to travel longer distances with the same amount of fuel, increasing the range of the vehicle and decreasing the frequency of refueling, making them more convenient and efficient for users (Yadav et al., 2017). Improved fuel economy often correlates with better acceleration and overall performance of vehicles (Thorat & Rao, 2011). Vehicle performance is often measured in terms of acceleration, speed, and handling, While engine power, vehicle mass, passenger or cargo capacity, and other parameters are not taken into account when measuring fuel economy, it is an imprecise indicator of energy efficiency (Hicks, 2014).

Aerodynamic drag is a force that opposes the motion of a vehicle through the air, caused by the shape of the vehicle and the friction of the air against the vehicle's surface (CFD Flow Engineering, 2023). It is estimated that aerodynamic drag accounts for about 20% of the fuel consumed by a vehicle, and at freeway speeds, it accounts for more than half of the fuel used (Cengel & Cimbala, 2006). Therefore, reducing aerodynamic drag can significantly improve fuel efficiency (Arteaga et al., 2020).

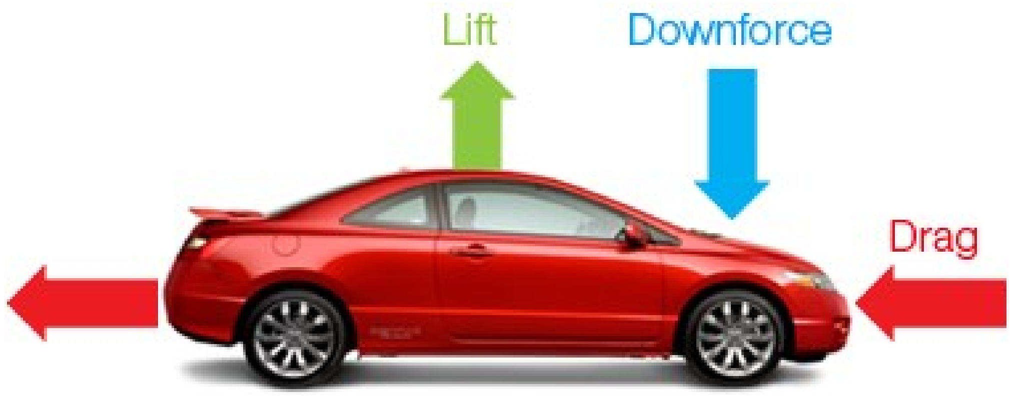

Figure 1.1: Areas of vehicle with different aerodynamic forces (Karthik, 2015)

Automakers can reduce aerodynamic drag by designing vehicles with smooth, flowing lines, rounded edges at the front of the vehicle, streamlined fairings, and improved trailer designs (Bayindirli & Celik, 2022). They can also use features such as spoilers, undertrays, and wheel covers on both the vehicle and trailer wheels to reduce drag (Karthik, 2015). In highway applications, 50% of total fuel economy is attributed to aerodynamics, making it crucial for vehicle manufacturers to optimize aerodynamics and reduce drag (Ahmed & Chacko, 2012).

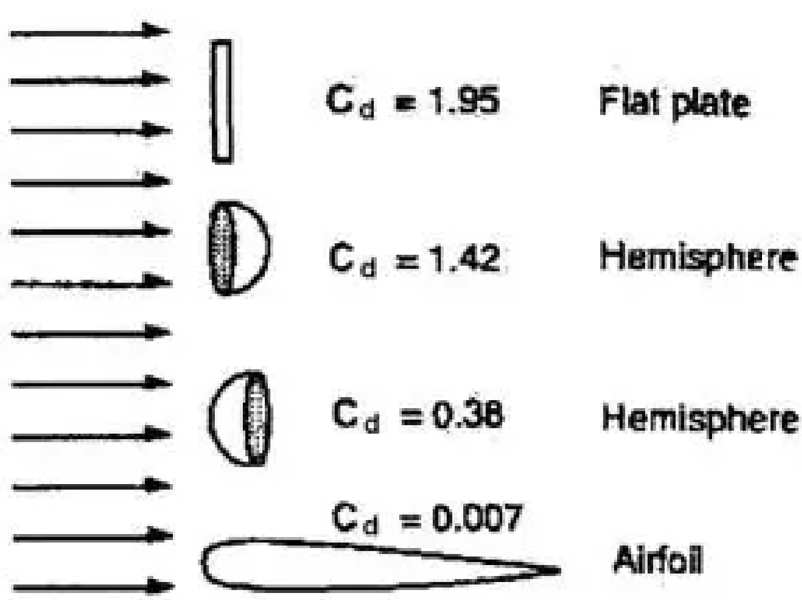

Figure 1.2: Typical Drag Coefficients of Various Body (CFD Flow Engineering, 2023)

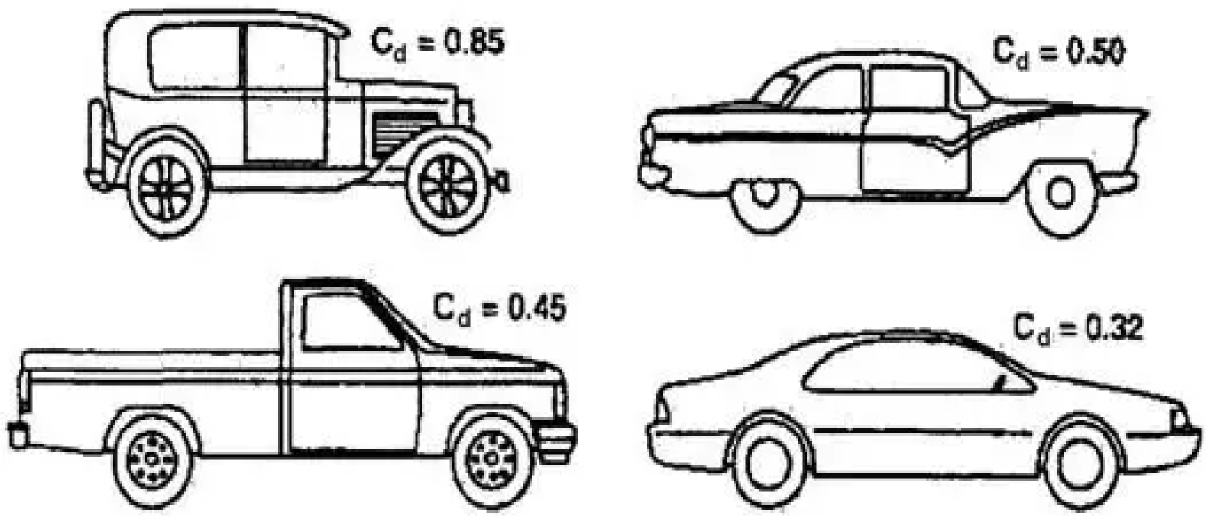

Figure 1.3: Typical Drag Coefficients of Various Car Body (CFD Flow Engineering, 2023)

The Anbessa Intercity Bus is a widely-used means of transportation in Ethiopia. The service is provided in Addis Ababa by the government controlled Anbessa City Bus Services Enterprise (ACBSE). With various sizes and configurations available, the most common model is a 50-seater with a 12-meter wheelbase (Anbassa City Bus Service Enterprise, 2014). Despite its long service history, the Anbessa Intercity Bus has very poor external body shape, as shown in *Figure 1.4*, and hence has very high aerodynamic drag that significantly increases its fuel consumption as it moves. The frontal shape of the bus is a vertical rectangular structure which creates a very high aerodynamic drag at high speeds. Its current design poses limitations such as a high windshield angle, which increases aerodynamic drag and thus reduces fuel efficiency.

The windshield angle, which is the angle at which the windshield is tilted relative to the horizontal ground plane, of vehicles plays a crucial role in vehicle aerodynamics and fuel consumption (Abdellah & Bo, 2017). It significantly affects the amount of drag experienced by the vehicle (Bayındırlı & Çelik, 2020). It directly influences the flow of air around the vehicle, affecting aerodynamic drag (Vignesh et al., 2019). The potential impact of windshield angle on fuel consumption is significant. According to a study by the National Renewable

Energy Laboratory (NREL), even a 1° reduction in windshield angle can improve fuel efficiency by up to 0.5% (Hicks, 2014).

Figure 1.4: Anbessa City Bus (Anbassa City Bus Service Enterprise, 2014)

Variations in windshield angle have a significant impact on the flow of air around a vehicle, which in turn affects drag and fuel efficiency. A tilted windshield deflects the airflow over the top of the vehicle, while a vertical windshield allows the airflow to hit the front of the vehicle directly. This difference in airflow can lead to substantial changes in drag and fuel efficiency (Hai-tao, 2012). For instance, a study by the University of Michigan found that reducing the windshield angle by 5° can reduce drag by up to 3%, resulting in a notable improvement in fuel efficiency (Bechtold & Regency, 2018). Manufacturers consider windshield angle as a critical factor in optimizing vehicle aerodynamics and fuel consumption. By adjusting the windshield angle, they can shape the airflow, minimize drag, and enhance fuel efficiency (Howell et al., 2021).

Additionally, windshield angle plays a role in vehicle stability and safety. It affects the vehicle's resistance to crosswinds, reducing the likelihood of destabilization at high speeds (Jeyasingham & Zhu, 2018). Properly angled windshields also optimize visibility for the driver, enhancing safety on the road (He et al., 2020). By considering the importance of windshield angle, manufacturers can create vehicles that offer improved fuel efficiency, stability, and safety (Abdellah & Bo, 2017).

By reducing the windshield angle of the Anbessa Intercity Bus, the drag force can be minimized, resulting in improved fuel efficiency. With a decreased angle, the airflow will be deflected over the top of the bus more smoothly, reducing the energy required to overcome drag (Yadav et al., 2017). This optimization can lead to substantial fuel savings and a reduced environmental impact. Additionally, a lower windshield angle can also contribute to enhanced stability, especially when encountering crosswinds during long-distance journeys (Karthik, 2015). Overall, studying and implementing measures to optimize the fuel economy of the Anbessa Intercity Bus can have far-reaching benefits, both economically and environmentally.

Since, Anbessa Intercity Bus is a popular mode of transportation in Ethiopia, used by millions of people each year, studying the fuel economy and optimization of the bus is relevant and beneficial (Anbassa City Bus Service Enterprise, 2014). Improving its fuel economy would result in significant fuel savings, reducing costs for transportation companies and passengers. Moreover, improving the fuel economy of the bus would have a positive environmental impact, as it is a major source of air pollution in Ethiopia. Enhancing fuel efficiency would help reduce emissions and minimize its environmental footprint.

1.2. Problem Statement

Anbessa Intercity Bus has very poor external body shape, and hence has very high aerodynamic drag that significantly increases its fuel consumption as it moves. The frontal shape of the bus is a vertical rectangular structure which creates a very high aerodynamic drag at high speeds. According to studies, a running vehicle's overall aerodynamic drag is made up of about 30% generated drag by a vortex in the back of the vehicle and about 70% pressure drag by stagnation on the front side of the vehicle. However, by reducing the windshield angle, the drag force can be minimized, resulting in improved fuel efficiency. Thus, this thesis aims to study the aerodynamic performances of the existing Anbessa Intercity Bus with special focus on the effects of the windshield angle on its fuel consumption. Moreover, possible optimizations of the frontal structures will be made to improve the fuel economy of the bus.

1.3. Research Question

This thesis is focused on the following research questions:

- What are the effects of various windshield angles on the aerodynamic drag of the Anbessa Intercity Bus?
- What is the impact of windshield angle on fuel economy for the Anbessa Intercity Bus?
- How can the windshield angle of the Anbessa Intercity Bus be optimized to enhance fuel economy?

1.4. Objective

1.4.1. General Objective

The general objective of this thesis is to conduct computational fluid dynamics analysis of the effects of windshield angle on fuel economy and optimization for the locally assembled Anbessa intercity bus.

1.4.2. Specific Objectives

The specific objectives are:

- To analyze the effects of various windshield angles on the aerodynamic drag of the Anbessa Intercity Bus using CFD simulations,
- To investigate the impact of windshield angle on fuel economy for the Anbessa Intercity Bus using CFD simulations, and
- To optimize the windshield angle of the Anbessa Intercity Bus for improved fuel economy based on the CFD analysis results.

1.5. Scope of the study

The scope of this study encompasses the analysis of various windshield angles and their effects on the aerodynamic drag and fuel economy of the Anbessa Intercity Bus. The thesis will utilize CFD simulations to investigate the relationship between windshield angles and aerodynamic drag, providing insights into how different angles impact the overall performance of the bus.

Additionally, the study will explore the impact of windshield angle on fuel economy by examining the correlation between these variables. Furthermore, the thesis aims to optimize the windshield angle based on the CFD analysis results, suggesting potential adjustments that can improve the fuel efficiency of the bus. The study is limited to the Anbessa Intercity Bus and does not consider other types of buses or vehicles.

1.6. Significance of the Study

The significance of this study lies in its potential to improve the fuel economy and sustainability of public transportation systems. By analyzing the effects of various windshield angles on the aerodynamic drag and fuel economy of the Anbessa Intercity Bus, the study can identify the optimal windshield angle that can improve the fuel efficiency of the bus. This can lead to reduced operating costs for the bus operator and lower emissions of harmful exhaust gases, contributing to a cleaner and healthier environment. The study can also provide valuable information for bus manufacturers and policymakers to design and regulate more fuel-efficient and environmentally friendly vehicles. The findings of this study can be used to inform the design of future buses, leading to more sustainable and healthy communities through integrating mobility simulations in the urban design process.

1.7. Organization of the thesis

This thesis work is divided into six chapters. The first chapter provides a brief introduction to the concept of drag force, as well as factor that affect fuel efficiency of buses. Problem statement, objectives of the study, significance of the study, scope of the study and the expected result of the study are also presented in the first chapter. Whereas, the second chapter of the thesis is devoted to presenting a review of the recent literature in the area. In addition, the identified research gap is included in this chapter. Chapter three describes the required materials, tools, methods and methodology utilized for this thesis. A flow chart is also provided to show the working pattern and flow of the thesis. This chapter offers a detailed description of the steps taken to complete this thesis. Moreover, the conceptual design of windshield angle and its effect on the fuel economy. Furthermore, it includes CFD analysis of the effects of windshield angle on fuel economy and optimization for the locally assembled Anbessa Intercity Bus. And, the fourth chapter of the thesis discusses the results of chapter three. Finally, the fifth chapter of the thesis presents conclusions and recommendations based on the insights gained from chapter five.

CHAPTER TWO

2. LITERATURE REVIEW

2.1. Fuel Economy and Vehicle Performance

When purchasing a vehicle, fuel economy and vehicle performance are important factors to consider (Ali et al., 2017). Fuel economy refers to the amount of fuel consumed per distance traveled, while vehicle performance encompasses acceleration, handling, and maneuverability. Several factors influence fuel economy, including aerodynamics, vehicle weight, engine efficiency, driving conditions, and vehicle maintenance. Whereas, vehicle performance is influenced by factors such as engine power, vehicle weight, drivetrain, and suspension (Cengel & Cimbala, 2006). More powerful engines allow for faster acceleration and higher top speeds, while heavier vehicles may have slower acceleration and lower top speeds (Goney, 2017).

It's critical to weigh the trade-off between fuel economy and vehicle performance when selecting a car (Cengel & Cimbala, 2006). Less fuel-efficient cars are often those with larger engines, faster top speeds, all-wheel drive, and stronger suspensions. A car with an aerodynamic shape, lightweight construction, and a fuel-efficient engine should be selected if fuel efficiency is the main consideration. On the other hand, a car with a strong engine and a sporty suspension should be selected if driving performance is your main concern (Hai-tao, 2012). In the end, personal priorities will determine which is more important: vehicle performance or fuel economy (He et al., 2020).

Streamlined designs with features such as sloping roofs, smooth body contours, and aerodynamic side mirrors reduce drag and improve fuel efficiency by minimizing the energy required to overcome air resistance (Anderson, 2011). Fuel economy is increased with lighter cars since they use less energy to accelerate and maintain their current speed (Zolet et al., 2018). Driving conditions such as frequent stop-and-go traffic, aggressive acceleration, and excessive idling can significantly reduce fuel efficiency (White, 2011). Proper tire maintenance, including proper inflation and alignment, can improve fuel economy by reducing friction between the tires and the road (Parmar, 2016). Vehicles equipped with advanced transmissions, such as continuously variable transmissions (CVTs) or dual-clutch transmissions (DCTs), can provide better power delivery and optimize gear ratios for improved fuel efficiency (Juhala, 2014). The type of fuel used also impacts fuel economy and vehicle performance (Jeyasingham & Zhu, 2018).

(Berry, 2010) carried out research on how driving technique and vehicle performance affect conventional vehicles' actual fuel usage. She conducted two types of analysis to determine how driving style and vehicle performance affect conventional vehicles' actual fuel consumption. The study found that driving style can have a significant impact on fuel consumption, and adopting smoother driving techniques can help optimize fuel efficiency.

(Li et al., 2018) carried out research on how changes in vehicle gaps affected the Automatic Cruise Control (ACC) strategy's fuel efficiency and pollution performance. The study discovered that the vehicle gap had an impact on traffic flow fuel economy and that 1.5 s was the ideal vehicle gap. They suggest that the vehicle gap can have a significant impact on fuel economy, and optimizing the vehicle gap can help improve fuel efficiency in traffic flow.

(J. Wu et al., 2021) carried out research on the trade-offs between performance and fuel economy in vehicles: Evidence from diverse Chinese enterprises. According to the study, there is a trade-off between vehicle performance and fuel economy, meaning that advancements in vehicle technology may result in a decrease in fuel efficiency. The study analyzed data from 1,000 Chinese automobile manufacturers and found that firms with higher performance vehicles tend to have lower fuel economy. The study suggests that firms need to consider the trade-off between vehicle performance and fuel economy when designing vehicles to improve fuel efficiency. The study emphasizes the importance of considering the trade-off between vehicle performance and fuel economy when designing vehicles to improve fuel efficiency.

(Oh et al., 2020), based on engine fuel consumption maps and vehicle dynamics, studied how car specifications affect fuel economy. Using the Automatic Vehicle Location (AVL) commercial program, the study examined ten passenger cars and performed vehicle dynamic modeling on gasoline and diesel automobiles. The study found that the vehicle specifications, such as the engine fuel consumption map and vehicle dynamics, have a significant impact on fuel economy. The study suggests that vehicle specifications need to be considered when designing vehicles to improve fuel efficiency.

2.2. Aerodynamics in vehicles

Aerodynamics is the study of how air flows around objects and the forces it exerts on them (Anderson, 2011). It studies the relationship between vehicles and the air they move through (White, 2011). Predicting variations in pressure and velocity around different wing and body configurations requires a thorough understanding of aerodynamics. Aerodynamics is a major factor in how cars are designed and how well they operate (Anderson, 2011). Aerodynamically constructed vehicles have reduced drag, which means they will need less energy to move through the air, improving performance and fuel efficiency (Cengel & Cimbala, 2006).

Aerodynamics plays a significant role in vehicle performance, fuel efficiency, and overall stability on the road (Anderson, 2011). A vehicle with good aerodynamics experiences reduced drag, allowing it to move through the air more efficiently, resulting in improved fuel economy, reduced wind noise, and higher top speeds (Cengel & Cimbala, 2006). Properly designed aerodynamic features, such as spoilers and diffusers, can help generate downforce, improving traction and allowing vehicles to maintain stability at higher speeds and during cornering (Anderson, 2011).

Aerodynamic drag is a major determinant of fuel efficiency (Cengel & Cimbala, 2006). Because it will create less drag, a more aerodynamic vehicle will need less fuel to cover the same distance (Abdellah & Bo, 2017). Top speed is also influenced by aerodynamic drag; a vehicle with greater aerodynamics will reach its maximum speed faster due to reduced air resistance (Ahmed & Chacko, 2012). In general, wind noise will be reduced in a vehicle with greater aerodynamics. Furthermore, because it will produce more downforce and less lift at high speeds, a vehicle with greater aerodynamic efficiency will also be more stable. This can enhance handling and lower the possibility of accidents (Ali et al., 2017).

Automotive engineers use various techniques to improve the aerodynamic efficiency of vehicles. These techniques include streamlining, reducing frontal area, adding aerodynamic components, reducing weight and improving engine efficiency (Bayindirli & Celik, 2022).

Streamlining involves shaping the vehicle's body to reduce drag, while reducing frontal area involves minimizing the size of the vehicle's front end (Anderson, 2011). Adding aerodynamic components such as spoilers, wings, and diffusers can generate downforce and reduce drag (White, 2011). Reducing the weight of the vehicle can also improve its aerodynamics, as a lighter vehicle requires less power to maintain a given speed (L. L. Wu et al., 2020). Finally, improving engine efficiency can reduce fuel consumption and improve the vehicle's aerodynamics. By integrating these design elements, vehicle designers optimize aerodynamics and contribute to overall performance and efficiency (Yadav et al., 2017).

Evaluation of vehicle aerodynamics is a continuous process that may include wind tunnel experimentation and computer modeling to comprehend and enhance a variety of aspects of vehicle performance (Zolet et al., 2018). Automotive aerodynamics studied through wind tunnel testing includes putting a scale model of a car in a wind tunnel and measuring the forces acting on it while air flows over it (Vignesh et al., 2019). Wind tunnels are occasionally fitted with a rolling road to replicate the motion of the vehicle's wheels and guarantee precise findings. Automotive engineers can improve the performance, efficiency, and overall usefulness of automobiles by optimizing their designs with the help of these strategies (Cengel & Cimbala, 2006).

2.3. Windshield Angle and Aerodynamics

Windshield angle is one of the many factors that affect the aerodynamics of a vehicle (Vignesh et al., 2019). The windshield is a large, flat surface that is located at the front of the vehicle (Luong, 2022). The airflow over and around the windshield is necessary for the vehicle to move forward, and the angle of the windshield may have an impact on this movement (Kremheller, 2018). A more slanted windshield will lessen drag, which is the force generated by the air resistance the vehicle experiences as it drives ahead and opposes its forward motion (Arteaga et al., 2020). As the first part of the car to come into contact with approaching air, the windshield angle influences all aspects of the air flow surrounding the car, including drag, lift, and turbulence (Bayindirli & Celik, 2022).

The angle of the windshield can affect the amount of drag and lift that a vehicle experiences (Bayındırlı & Çelik, 2020). When the windshield angle is steep, the air is forced to change direction abruptly as it hits the windshield, causing an increase in drag. A more upright windshield angle can increase drag, while a more sloped angle can decrease drag (Elrawemi & Aburawey, 2019). Conversely, a more streamlined windshield angle, with a gentle slope, allows the air to smoothly flow over the vehicle's surface, reducing the drag. Lower drag leads to improved fuel efficiency and better overall aerodynamic performance (Goney, 2017).

The angle of a vehicle's windshield has a significant impact on lift, stability, and turbulence (Hai-tao, 2012). A steep windshield angle can create an upward pressure on the front of the vehicle, increasing lift, which can negatively impact stability, especially at higher speeds (He et al., 2020). On the other hand, a more streamlined windshield angle helps in reducing lift by allowing the air to flow smoothly over the vehicle's surface, resulting in improved stability (Howell et al., 2021). Turbulence is another factor affected by windshield angle. When the air encounters a steep windshield, it tends to create turbulence as it changes direction suddenly, which can disrupt the flow of air over the rest of the vehicle, leading to increased drag and reduced aerodynamic efficiency (Abdellah & Bo, 2017).

Depending on the type of car and how it will be used, different vehicles have different optimal windshield angles (Zolet et al., 2018). While SUVs and trucks may have a more upright windshield to improve visibility and handle their greater size, sports cars sometimes have a lower windshield angle to emphasize their sleek design and high-speed performance (Yadav et al., 2017). Studies have demonstrated that variations in windshield angle can significantly affect aerodynamic drag. Windshield angle is frequently tuned for drag reduction in automobiles (Ahmed & Chacko, 2012). Vehicle windshields are frequently designed with angles between -30 and -50 degrees for aerodynamic drag considerations (Arteaga et al., 2020). As a result, increasing the windshield angle by 1 degree can reduce the drag coefficient by around 0.4% (Parmar, 2016).

The optimal windshield inclination angle depends on several factors, including vehicle speed, vehicle shape, wind conditions, and the desired balance between aerodynamics and aesthetics (Muthuvel et al., 2013). When determining the optimal windshield inclination angle, factors such as minimizing the drag coefficient of the vehicle, providing adequate visibility for the driver, ensuring the structural strength of the windshield, and being cost-effective should be considered (Thorat & Rao, 2011). Increasing the windshield inclination angle can reduce the drag coefficient of a vehicle, but the reduction is not linear (Kremheller, 2018). For example, a more upright windshield angle may be preferred for a vehicle that is designed for off-road use, where aerodynamic performance is less important than visibility and durability (Luong, 2022).

Various automotive manufacturers have invested considerable effort in optimizing windshield inclination angles (Ahmed & Chacko, 2012). Companies like Tesla, BMW, and Audi have incorporated aerodynamic design principles to enhance fuel efficiency in their electric and hybrid vehicles (Howell et al., 2021). Tesla Model S, Toyota Prius, Honda Civic, Ford F-150, and Toyota Tacoma have 60°, 55°, 50°, 45° and 40° windshield inclination angle, respectively (Zhang et al., 2022).

Better fuel economy, lower pollutants, and enhanced vehicle performance are just a few advantages of optimizing an automobile's windscreen angle (Abdellah & Bo, 2017). Increased fuel efficiency and less drag can be achieved, particularly at high speeds, with the aid of an aerodynamic windshield (Cengel & Cimbala, 2006). However, optimizing the windshield angle for fuel economy can have some potential drawbacks. These include reduced driver visibility, especially for vehicles used in off-road or other demanding driving conditions, increased noise levels inside the vehicle, and increased cost due to the use of special materials or manufacturing techniques (Ghurri et al., 2023).

Several researchers have conducted studies on the effect of windshield angle of vehicles on fuel economy. (Bayındırlı & Çelik, 2020) conducted a study on the effect of windshield inclination angle on the drag coefficient of a bus model by CFD method. The study aimed to determine the effect of windshield angle on the performance and fuel consumption of buses. The researchers found that increasing the windshield angle decreased the drag coefficient, which in turn decreased fuel consumption. The study found that increasing the windshield angle by 1 degree resulted in a 0.4% reduction in drag. On buses, the inclination angle of the windshield has a significant impact on drag forces.

(Abdellah & Bo, 2017) conducted a study on windscreen angle and hood inclination optimization for drag reduction in cars. The study aimed to optimize the windscreen angle and hood inclination to reduce drag in cars, which would lead to a reduction in fuel consumption and emissions. The researchers found that optimizing the windscreen angle and hood inclination could reduce drag and improve fuel economy. The study showed that with only hood inclination change, the drag could be reduced considerably. The study also found that hood inclination needs to be adjusted for the least amount of drag. Better aerodynamic car designs result in less gasoline being used, which lowers the emissions from the vehicle.

(Hai-tao, 2012) conducted a study on the effect of windscreen angles on car characteristics. The study used a computational model to simulate the flow movement outside the automobile with different windscreen angles. The researchers found that the coefficients of aerodynamic resistance were not a linear function with car rear windscreen angles. The coefficients of aerodynamic resistance dropped at small rear windscreen angles and increased greatly from 25 to 45 degrees. The study showed that the results could provide a useful reference for the design of passenger cars and had certain guiding significance for practical application

Windshield angle can have a significant impact on aerodynamic drag, with reductions of up to 10% possible for certain vehicle types, according to a comprehensive study conducted by the National Renewable Energy Laboratory (NREL) in the United States (Pershing & Masaki, 1976). Another study by researchers at the University of Michigan found that a 10-degree increase in windshield angle can reduce aerodynamic drag by up to 5%, and that the impact of windshield angle on aerodynamic drag is most significant at high speeds. The reduction in drag due to better aerodynamic design of cars can reduce fuel consumption and emissions (Cakir, 2012).

(Damissie & Babu, 2017) conducted a study to investigate the flow around Yutong cross-country bus, which is assembled at Bishoftu Automotive Industry, to reduce the drag force. They used ANSYS Fluent to conduct the analysis at inlet air speeds of 23.1 m/s, 27.78 m/s, and 31.94 m/s. They modified the windshield angle of the bus, and with the new model, he claimed to reduce the drag force of the bus by 39.4% compared to the original model

(Vignesh et al., 2019) used ANSYS fluent to study the effects of hood and windshield inclination angle on aerodynamic drag of passenger car with the aim of improving its fuel economy. The CFD analysis was conducted at inlet air velocity of 25 km/h at various hood and windshield angles. They concluded that 32 ° back windscreen angle gives the minimum CD. The front windscreen angle should be below 45° for minimum drag and CD decreases linearly as hood inclination increases.

(Korkut & Gören, 2020) studied the advantages of using side mirrors or cameras for developing the aerodynamic structure of Solaris 7. When the Solaris 7 did not have a mirror and a camera, its drag coefficient was 0.0919. When it had side mirrors but no camera, the drag coefficient was 0.13. When it had a camera but no side mirrors, the drag coefficient was 0.1137. In this instance, the drag coefficient was increasing in tandem with the energy consumption. The drag coefficient of the Solaris 7 solar car increased by 42% when the side mirrors were used, and by 23.72% when the rearview camera was installed. They found that using a camera is more effective than using a side mirror.

(Cakir, 2012) studied the influence of rear spoiler inclination angle on the generated lift, drag, and pressure distributions using Autodesk Simulation CFD software. Rear spoilers redirect the airflow behind the vehicle & increase the negative lift of the vehicle. In the investigation, six modifications were simulated, while the 12-degree spoiler inclination angle model was found to be the most optimum though it created 1.56% extra CD than 4-degree inclination angle.

2.4. Conceptual Design of Windshield Angle

The windshield angle of vehicles plays a crucial role in vehicle aerodynamics and fuel consumption. It significantly influences the flow of air around the vehicle, affecting its aerodynamic drag (Vignesh et al., 2019). A tilted windshield deflects the airflow over the top of the vehicle, while a vertical windshield allows the airflow to hit the front of the vehicle directly (Jeyasingham & Zhu, 2018). As such, in order to design and model the windshield of a vehicle from the aerodynamic point of view, various governing equation such as continuity equation, motion equation, turbulence modeling, and viscous model can be utilized. Here's an overview of the relevant equations and models.

2.4.1. Continuity Equation

The continuity equation is a fundamental equation in fluid dynamics that represents the conservation of mass (Cengel & Cimbala, 2006). It states that the mass entering a control volume must equal the mass leaving the control volume, accounting for any accumulation within the system (Anderson, 2011). In the context of the windshield design, the continuity equation is essential for understanding how the airflow around the bus is affected by the windshield angle. It ensures that there is no accumulation or depletion of mass within the airflow around the bus. This equation helps maintain a balanced flow and is essential for accurate aerodynamic analysis. Mathematically, it can be expressed as (White, 2011):

$$\frac{\partial \rho}{\partial t} + \nabla.(\rho U) = 0 \qquad \text{Equation 2.1}$$

Where,

- ρ is the density of the fluid (Kg/m^3),
- t is time (s),
- U is the velocity vector (m/s), and
- ∇ is the gradient operator.

Moreover, continuity equation can be expressed in detail as (White, 2011):

$$\frac{\partial \rho}{\partial t} + \frac{\partial (\rho u)}{\partial x} + \frac{\partial (\rho v)}{\partial y} + \frac{\partial (\rho w)}{\partial z} = 0 \qquad \text{Equation 2.2}$$

Where,

- ρ is the density of the fluid (Kg/m^3),
- t is time (s),
- u, v, w are the velocity vector in x, y and z directions, respectively (m/s).

Figure 2.1: Direction of vehicle movement

Furthermore, since the vehicle moves in one direction, as shown in *Figure 2.1*, considering this direction as x direction, velocity along y and z directions can be neglected compared to the x direction. In addition, it can be considered that the fluid property will not change with time, the continuity equation can be expressed as:

$$\frac{\partial(\rho u)}{\partial x} = 0 \qquad \text{Equation 2.3}$$

Where,

- ρ is the density of the fluid (Kg/m^3), and
- u is the velocity vector in x direction (m/s).

2.4.2. Motion Equation

In the context of windshield angle design, the motion equation is used to model the airflow around the bus and predict how changes in the windshield angle will affect the flow patterns and drag coefficients. The motion equation, also known as the momentum equation, describes the relationship between the forces acting on a fluid and the resulting motion. The Navier-Stokes equation is used to describe the motion of fluid and are fundamental to fluid dynamics. It accounts for the effects of pressure, viscosity, and external forces on the fluid flow. It consists of three equations for the conservation of momentum in the three spatial directions. It can be expressed as (Cengel & Cimbala, 2006):

$$\rho\left(\frac{\partial U}{\partial t} + U.\nabla U\right) = \mu\nabla^2 U - \nabla P + \rho g_x \qquad \text{Equation 2.4}$$

Where,

- ρ is the density of the fluid (Kg/m^3),
- t is time (s),
- U is the velocity vector (m/s),

- μ is the dynamic viscosity,
- P is the pressure (N/m^2),
- g is the gravitational acceleration vector (m/s^2), and
- ∇ is the gradient operator.

Moreover, the momentum equation can be expressed for x, y and z directions, respectively, in detail as (White, 2011):

Equation 2.5

$$\rho\left(\frac{\partial \mathrm{u}}{\partial \mathrm{t}}+u\frac{\partial \mathrm{u}}{\partial \mathrm{x}}+v\frac{\partial \mathrm{u}}{\partial \mathrm{y}}+w\frac{\partial \mathrm{u}}{\partial \mathrm{z}}\right)=\mu\left(\frac{\partial^2 \mathrm{u}}{\partial \mathrm{x}^2}+\frac{\partial^2 \mathrm{u}}{\partial \mathrm{y}^2}+\frac{\partial^2 \mathrm{u}}{\partial \mathrm{z}^2}\right)-\frac{\partial \mathrm{P}}{\partial \mathrm{x}}+\rho g_x$$

$$\rho\left(\frac{\partial \mathrm{v}}{\partial \mathrm{t}}+u\frac{\partial \mathrm{v}}{\partial \mathrm{x}}+v\frac{\partial \mathrm{v}}{\partial \mathrm{y}}+w\frac{\partial \mathrm{v}}{\partial \mathrm{z}}\right)=\mu\left(\frac{\partial^2 \mathrm{v}}{\partial \mathrm{x}^2}+\frac{\partial^2 \mathrm{v}}{\partial \mathrm{y}^2}+\frac{\partial^2 \mathrm{v}}{\partial \mathrm{z}^2}\right)-\frac{\partial \mathrm{P}}{\partial \mathrm{y}}+\rho g_y$$

$$\rho\left(\frac{\partial \mathrm{w}}{\partial \mathrm{t}}+u\frac{\partial \mathrm{w}}{\partial \mathrm{x}}+v\frac{\partial \mathrm{w}}{\partial \mathrm{y}}+w\frac{\partial \mathrm{w}}{\partial \mathrm{z}}\right)=\mu\left(\frac{\partial^2 \mathrm{w}}{\partial \mathrm{x}^2}+\frac{\partial^2 \mathrm{w}}{\partial \mathrm{y}^2}+\frac{\partial^2 \mathrm{w}}{\partial \mathrm{z}^2}\right)-\frac{\partial \mathrm{P}}{\partial \mathrm{w}}+\rho g_w$$

Where,

- ρ is the density of the fluid (Kg/m^3),
- t is time (s),
- u, v, w are the velocity vector in x, y and z directions, respectively (m/s).
- μ is the dynamic viscosity,
- P is the pressure (N/m^2), and
- g is the gravitational acceleration vector (m/s^2).

Furthermore, as *shown in Figure 2.1*, since the vehicle moves in one direction, considering this direction as x direction, momentum along y and z directions can be neglected compared to the x direction. In addition, there is no gravity vector along x direction. Thus, the momentum equation can be expressed as:

Equation 2.6

$$\rho\left(\frac{\partial \mathrm{u}}{\partial \mathrm{t}}+u\frac{\partial \mathrm{u}}{\partial \mathrm{x}}\right)=\mu\left(\frac{\partial u_i}{\partial x_j}+\frac{\partial u_j}{\partial x_i}\right)-\frac{\partial \mathrm{P}}{\partial \mathrm{x}}$$

Where,

- ρ is the density of the fluid (Kg/m^3),
- t is time (s),
- u is the velocity vector in x direction (m/s),
- μ is the dynamic viscosity, and
- P is the pressure (N/m^2).

2.4.3. Turbulence modeling

Turbulence refers to unpredictable motion of fluid flow characterized by chaotic and irregular fluctuations in the flow (White, 2011). Turbulence models are employed to simulate the effects of turbulence in the fluid flow, as solving the Navier-Stokes equations directly for turbulent flows is computationally expensive (Muthuvel et al., 2013). These models introduce additional equations to represent turbulent kinetic energy (k), its dissipation rate (ε), or its specific dissipation rate (ω). To accurately simulate turbulent flows, turbulence models are employed. Common turbulence models include (Qu & Xie, 2021; Zolet et al., 2018):

- Standard $k-\varepsilon$ turbulence model
- Realizable $k-\varepsilon$ turbulence model
- Standard $k-\omega$ turbulence model
- Shear stress transport $k-\omega$ turbulence model
- Reynolds-averaged Navier-Stokes (RANS) equations, and
- Large eddy simulation (LES)

In the context of the windshield angle design, accurate modeling of turbulence is crucial for capturing the complex airflow patterns around the vehicle. These models help in understanding the impact of turbulence on drag coefficients and fuel consumption. One of the most used turbulence models is the conventional k-ε model, which is two equations of the flow plus two additional transport equations to capture the turbulent properties of the flow (Zolet et al., 2018). The anticipated flow is turbulent and thoroughly characterized. There is very little impact from molecular viscosity. Even so, because of this model's shortcomings, it performs poorly, particularly when there are significant adverse pressure gradients (Thorat & Rao, 2011). The Standard $k-\varepsilon$ turbulence model It contains a two-equation model that transfers equations to depict the flow's turbulent characteristics. Turbulent kinetic energy (k) is the first transferred variable, while turbulent dissipation (ε) is the second.

Turbulent kinetic energy in standard $k - \varepsilon$ turbulence model is given by (Hai-tao, 2012),

Equation 2.7

$$\frac{\partial}{\partial \mathrm{t}}(\rho k) + \frac{\partial}{\partial x_i}(\rho u_i k) = \frac{\partial}{\partial x_j}\left[(\mu + \mu_t)\frac{\partial k}{\partial x_j}\right] + G - \rho\varepsilon$$

Where,

- ρ is the density of the fluid (Kg/m^3),
- t is time (s),
- k is turbulent kinetic energy (J),
- u_i is the velocity vector in x_i direction (m/s),
- μ is the dynamic viscosity,
- μ_t is turbulent viscosity,
- ε is the turbulent kinetic energy dissipation rate, and
- G is the generation term of turbulent kinetic energy caused by velocity gradient.

The turbulent viscosity, μ_t in *Equation 2.7,* is given by (Hai-tao, 2012):

Equation 2.8

$$\mu_t = 0.09\rho\frac{k^2}{\varepsilon}$$

Where,

- μ_t is turbulent viscosity,
- ρ is the density of the fluid (Kg/m^3),
- k is turbulent kinetic energy (J), and
- ε is the turbulent kinetic energy dissipation rate.

Moreover, the generation term of turbulent kinetic energy caused by velocity gradient, G in *Equation 2.7,* is given by (Hai-tao, 2012):

$$G = \mu_t \left[\frac{\partial u_i}{\partial x_j} + \frac{\partial u_j}{\partial x_i}\right]\frac{\partial u_i}{\partial x_j}$$ Equation 2.9

Where,

- G is the generation term of turbulent kinetic energy caused by velocity gradient,
- μ_t is turbulent viscosity,
- u_i is the velocity vector in x_i direction (m/s), and
- u_j is the velocity vector in x_j direction (m/s).

Turbulent dissipation rate in standard $k - \varepsilon$ turbulence model is given by: (Hai-tao, 2012)

$$\frac{\partial}{\partial \mathrm{t}}(\rho\varepsilon) + \frac{\partial}{\partial x_i}(\rho u_i \varepsilon) = \frac{\partial}{\partial x_j}\left[(\mu + \mu_t)\frac{\partial \varepsilon}{\partial x_j}\right] + 1.44\frac{\varepsilon}{k}G - 1.92\rho\frac{\varepsilon^2}{k}$$ Equation 2.10

Where,

- ρ is the density of the fluid (Kg/m^3),
- t is time (s),
- ε is the turbulent kinetic energy dissipation rate
- k is turbulent kinetic energy (J),
- u_i is the velocity vector in x_i direction (m/s),
- μ is the dynamic viscosity,
- μ_t is turbulent viscosity, and
- G is the generation term of turbulent kinetic energy caused by velocity gradient.

2.4.4. Viscous Modeling

The viscous model accounts for the effect of viscosity, which is the resistance of a fluid to deformation. The most common viscous model is the Newtonian model, which assumes that the shear stress is proportional to the strain rate. Mathematically, it can be expressed as (White, 2011):

$$\tau = \mu \nabla \mathrm{U}$$ Equation 2.11

Where,

- τ is the shear stress (Pa),
- μ is the dynamic viscosity
- ∇ is the gradient operator, and
- U is the velocity vector in (m/s).

2.4.5. Aerodynamic Characteristics

Aerodynamics is the study of how moving objects interact with the air (Ghurri et al., 2023). As shown in *Figure 2.2*, several forces are applied to the vehicle in different directions when it is traveling at a high speed.

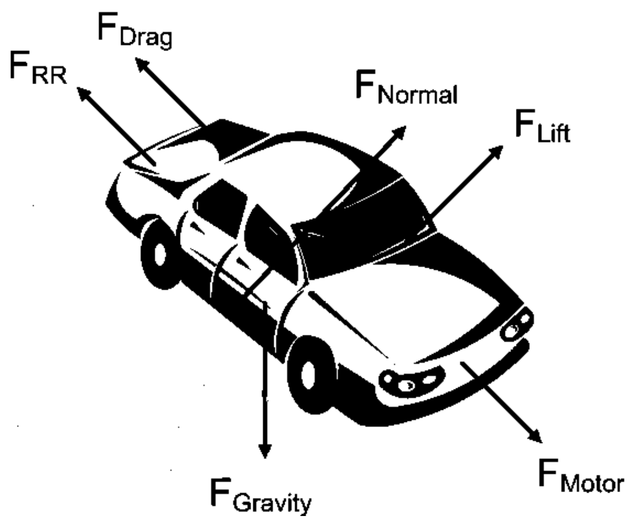

Figure 2.2: Forces acting on vehicle body (Cakir, 2012)

Aerodynamic drag consists of pressure drag and friction drag. About 90% of aerodynamic drag is created by pressure differential resistance and 10% of aerodynamic drag is created by friction resistance (Hui et al., 2020). Drag force can be determined from:

Equation 2.12

$$F_d = \frac{1}{2} C_D \rho A_f v^2$$

Where,

- F_d is the drag force (N),

- C_D is the drag coefficient,
- ρ is the density of the fluid,
- A_f is the frontal area (m^2), and
- v is the velocity of the fluid (m/s).

The separation of flow is the primary cause of the generation of drag force. Drag forces are produced by the separation of, which results in a pressure drop on the surface. According to Equation 2.12, the cross-sectional area is the one of the parameters that affect the results of the drag force. The drag coefficient will be greatly impacted by the airflow velocity and the vehicle's body form (Hui et al., 2020).

Whereas, when lift force is applied in a positive direction, the vehicle is lifted into the air; however, if lift force is applied in a negative direction, it may result in excessive wheel down force. (CFD Flow Engineering, 2023). To prevent using too much lift or down force, engineers work to keep this value within the necessary range. Lift force can be determined from:

Equation 2.13

$$F_L = \frac{1}{2} C_L \rho A_f v^2$$

Where,

- F_L is the lift force (N),
- C_L is the lift coefficient,
- ρ is the density of the fluid,
- A_f is the frontal area (m^2), and
- v is the velocity of the fluid (m/s).

2.4.6. Fuel economy

Fuel economy is of utmost importance in the automotive industry. Improved fuel efficiency translates to reduced fuel consumption, leading to significant cost savings for vehicle owners and operators (Bechtold & Regency, 2018). By using more efficient engines, lightweight materials, aerodynamic designs, and developing new technologies, automotive industry is constantly working to improve fuel economy (Bayindirli & Celik, 2022).

According to (Ghurri et al., 2023), the following equations can be used to express the relations between drag force and fuel consumption numerically. As such, the power required to overcome drag force is given by:

$$P = F_D v \qquad \text{Equation 2.14}$$

Where,

- P is the power required to overcome the drag (w),
- F_D is the drag force (N), and
- v is the air velocity (m/s).

The fuel efficiency of automobile is inversely proportional to the net amount of drag force acting it. Drag forces are the extra and unavoidable forces which act on the vehicle. Moreover, the energy consumption per Km-hour can be determined from:

$$E = \frac{P}{V_{Bus}} \qquad \text{Equation 2.15}$$

Where,

- E is the energy consumption per Km-hour (wh/Km),
- P is the power required to overcome the drag (w), and
- V_{Bus} is the velocity of the vehicle (m/s).

Furthermore, the vehicle's fuel consumption can be calculated by:

$$F_C = \frac{E}{\phi_d} \qquad \text{Equation 2.16}$$

Where,

- F_C is the fuel consumption (L/Km),
- E is the energy consumption per Km-hour (wh/Km), and
- ϕ_d is the specific energy of the fuel (Wh/L).

2.5. Research gap

Various literatures acknowledge the critical role of reducing drag in enhancing fuel economy. As such, various works have been done to improve fuel economy through reduction of drag coefficients. In addition, literatures discuss that windshields play a substantial role in drag generation. Thus, optimization of windshield angles to reduce the drag coefficients have been done, usually for automobiles. However, a comprehensive study on how altering the windshield angle of city buses can mitigate this issue and subsequently improve fuel economy remains limited. As such, still, various city buses and cross-country buses have suboptimal aerodynamic design, primarily owing to their vertical rectangular windshield configuration. And, this suboptimal design results in high aerodynamic drag, significantly increasing fuel consumption. One of such city buses is Anbessa city bus. Hence, this thesis seeks to bridge this gap by providing a systematic exploration of the impact of windshield angle on aerodynamic performance, thus aiming to contribute to the optimization of the Anbessa intercity bus's frontal design to enhance fuel efficiency.

CHAPTER THREE

3. MATERIALS AND METHODOLOGY

In order to improve fuel economy, various windshield angle of Anbessa intercity bus is investigated and CFD Analysis of the Effects of Windshield Angle on the aerodynamics of the vehicle is performed. The study emphasizes the model and analysis of Anbessa intercity bus using CFD tools considering various windshield inclination angle. Moreover, the optimization is performed for Anbessa intercity bus by considering factors such as aerodynamic drag, lift, and fuel economy. The methodology for design and modeling can be broken down into several steps. The key procedures followed in this study are represented in *Figure 3.1*.

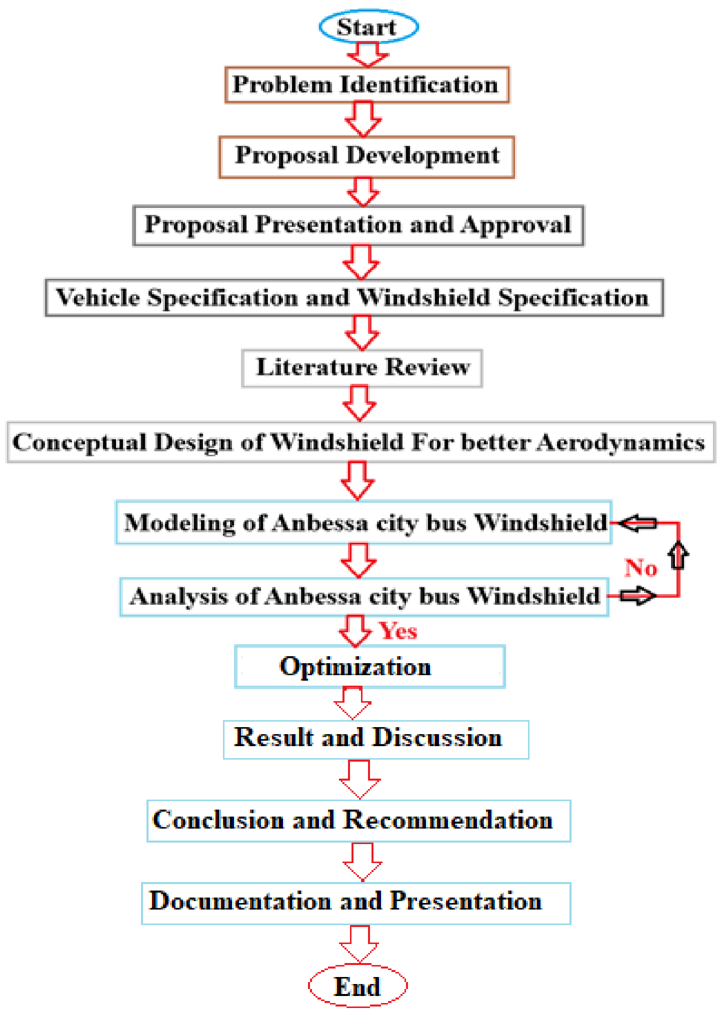

Figure 3.1: A Methodology flowchart

3.1. Research Design

This thesis focusses on CFD analysis of the effects of windshield angle on fuel economy and optimization for the locally assembled Anbessa intercity bus. The study uses a mixed-methods approach, combining quantitative and qualitative data collection methods. The quantitative data survey focusses to collect data on the general specification of the vehicle, and the dimensions of the vehicle's windshield. Therefore, data is collected from the manufacturer of the selected vehicle. The qualitative data focusing on the methods, approaches and procedures of the CFD analysis of the effects of windshield angle is collected through document review. The thesis identified the most feasible windshield angle of the selected vehicle based on the optimization. Moreover, the thesis investigated the effect of the windshield angle on aerodynamic drag and fuel economy.

3.2. Data Collection

In this thesis, a mixed-method approach is employed to collect data. The approach consists of two main methods: document review, and vehicle specification.

3.2.1. Document review

A comprehensive review of relevant literature and documents related to windshield inclination angle, aerodynamic drag and fuel economy are conducted. This encompasses studying literature on aerodynamics in vehicles, design and modeling of windshield inclination angle, and the effect of windshield angle on the fuel economy. In addition, the part catalogue of YUTONG BUS MODEL ZK6126HGA model, (Zhengzhou Yutong Group Co. Ltd, 2019) is consulted.

3.2.2. Vehicle Specification

For CFD analysis of the effects of windshield angle on fuel economy and optimization for the locally assembled Anbessa intercity bus, the specification of the selected vehicle and its windshield are required. Thus, the specifications of Anbessa lower floor bus like that of overall dimensions, fuel economy and the dimensions of the windshield are collected from the Bishoftu Automotive manufacturing industry of Ethio Engineering group. For this particular thesis, YUTONG Bus Model ZK6126HGA, shown in *Figure 3.2*, is considered for the CFD analysis of the effects of windshield angle on fuel economy. Hence, the specification shown in *Table 3.1* are collected accordingly.

Table 3.1: Specifications of YUTONG ZK6126HGA Bus (Ethio Engineering group, 2023)

S.No.	Parameter		Value
1	Length (mm)		12499
2	Width (mm)		2550
3	Height (mm)		3180
4	Interior height (mm)		2200
5	Wheelbase (mm)		6375
6	Ground clearance (mm)		170
7	Kerb Weight (Kg)		12050
8	Gross vehicle weight (kg)		21500
9	Seating Capacity		42
10	Standing Capacity		35
11	Maximum Speed (Km/h)		100
12	Fuel Tank Capacity (L)		250
13	Engine	Number of cylinders	6
		Displacement (Liter)	8
		Power (KW)	213.4 at 2200 RPM
		Torque (Nm)	1160 at 1200-1600 RPM
		Type of fuel	Diesel
		Fuel Economy (Km/Liter)	4.5

The windshield angle of a bus is typically measured from the vertical, with a larger angle indicating a more sloped windshield (Vignesh et al., 2019). The specific windshield angle for each bus model can vary depending on the manufacturer's design. As such, it is required to collect the specifications of windshield of the selected vehicle. Thus, the specifications of windshield of YUTONG ZK6126HGA bus is collected from Bishoftu Automotive manufacturing industry as shown in *Table 3.2*

Figure 3.2: YUTONG Bus Model ZK6126HGA (JingFu, 2023)

Table 3.2: Specification of YUTONG ZK6126HGA bus windshield (Ethio Engineering group, 2023)

S.No.	Parameter	Value
1	Material	Laminated safety glass
2	Width (m)	2
3	Height (m)	1.2
4	Angle (^{O})	19

Moreover, Anbessa city bus has over hundred routes and destination, *as shown in Appendix 2*. The maximum route length is 47.2 km from Deber Zeit to Legehar along Gotera. Whereas, the minimum route length is 7 km from Megenagna to Goro Sefera along Anbessa Garages.

3.3. Softwares Utilized for CAD Modeling, Analysis and Optimization

After the required specifications of the YUTONG ZK6126HGA bus model and its windshield are obtained through data collection, the software modeling of the current YUTONG ZK6126HGA bus model and modification of the vehicle's windshield inclination angle is performed using CAD and CFD softwares. This includes the 3D modeling of the model and its CFD analysis. As part of the CFD, 3D CAD models is developed, boundary conditions are applied, and the vehicle's velocity is applied to simulate the aerodynamic drag effect. SolidWorks 2022 is used for CAD modeling, and Phoenics software is used for CFD Analysis. Moreover, Microsoft Excel is used for plotting the chart based on the acquired result of the Phoenics software. Furthermore, DESIGN EXPERT 13 is used for optimization of the model.

SolidWorks is a widely-used Computer-Aided Design (CAD) software that is employed by millions of engineers worldwide (Solidworks, 2022). It is equipped with a comprehensive set of features and tools, enabling users to create drawings, perform design analysis, estimate costs, generate renderings, and create animations, among other functions (Capitol Technology University, 2019). Renowned for its user-friendly interface, extensive functionality, and broad range of capabilities, it has become a favored choice for engineers and designers across diverse industries and professions worldwide (Solidworks, 2022).

Phoenics software is a general-purpose CFD software that can be used to analyze and simulate a wide variety of fluid flow, heat transfer, and other related phenomena. The software analyzes the model based on the finite volume. It has the ability to model single-phase and multi-phase flows, heat transfer, chemical reactions, and particle tracking. Moreover, it has flexible geometry and mesh generation capabilities, and detailed post-processing and visualization tools (ACADS-BSG, 2024). Whereas, DESIGN EXPERT is a software program specifically designed to assist with experimental design and statistical analysis (Stat-Ease Inc, 2024). It offers a wide range of applications, from screening factors to optimizing product formulations.

With its array of advanced features including factorial, response surface, and mixture designs, DESIGN EXPERT software boasts advantages such as user-friendly design wizards, comprehensive analysis tools, and effective graphical outputs for communicating (Ritme, 2024).

MICROSOFT EXCEL, is a versatile spreadsheet software widely used for data analysis, calculation, and visualization. It has several applications ranging from simple data entry to sophisticated statistical analysis. With the aid of these features, users can compute correlation coefficients, carry out single and multiple regressions, and optimize solutions by establishing constraints and variables inside the program (Microsoft, 2024).

3.4. CAD Modeling of Anbessa Bus

For both the current model of Anbessa bus and the modification of the Anbessa bus windshield angle, SolidWorks software is used to create the 3D CAD modeling. Here, six models are created in SolidWorks. All the models have the same basic dimensions like height, width and length. Moreover, as shown in *Appendix 9* to *Appendix 13*, their basic parts like base, tire, rim, and etc. are the same. However, they have different windshield angle. As such the current model has a windshield angle of 19^{O}. Whereas, 25^{O}, 30^{O}, 35^{O}, 40^{O}, and 45^{O} windshield angle are considered for the modification of windshield angle of Anbessa bus, as shown in *Table 3.3*.

In order to create CAD model of current model of Anbessa bus, various dimensions such as length, width, height and windshield angle are required. Hence, based on the dimensions given in *Table 3.3*, the 3D CAD model of current model of Anbessa bus, created using SolidWorks software, is given in *Figure 3.3*. Moreover, the detail drawing of the model is shown in *Appendix 3*.

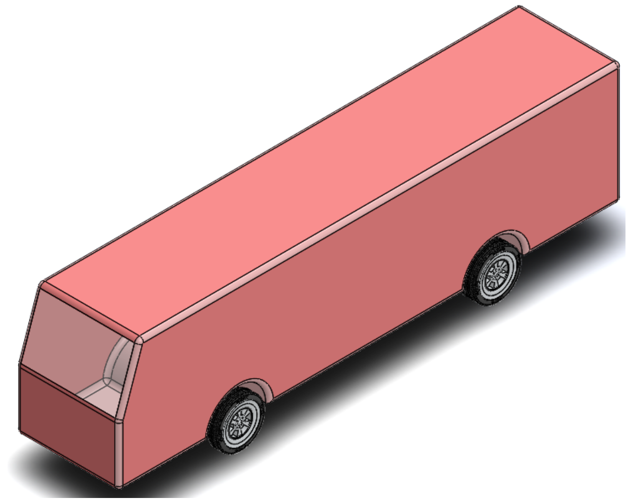

Figure 3.3: SolidWorks model snap assembly of simplified current model of Anbessa bus

Table 3.3: Summary of the dimensions of Various model of Anbessa bus

S.No.	Parameter	Model 1	Model 2	Model 3	Model 4	Model 5	Model 6
1	Length (mm)	12499	12499	12499	12499	12499	12499
2	Width (mm)	2550	2550	2550	2550	2550	2550
3	Height (mm)	3180	3180	3180	3180	3180	3180
4	Windshield Angle (^{O})	19	25	30	35	40	45

In order to create CAD model of the modified model of Anbessa bus, various dimensions such as length, width, height and windshield angle are required. Hence, based on the dimensions given in *Table 3.3*, the 3D CAD model of five new modified model of Anbessa bus, created using SolidWorks software, is given in *Figure 3.4*. Moreover, the detail drawings of the modified models are shown in *Appendix 4* up to *Appendix 8*.

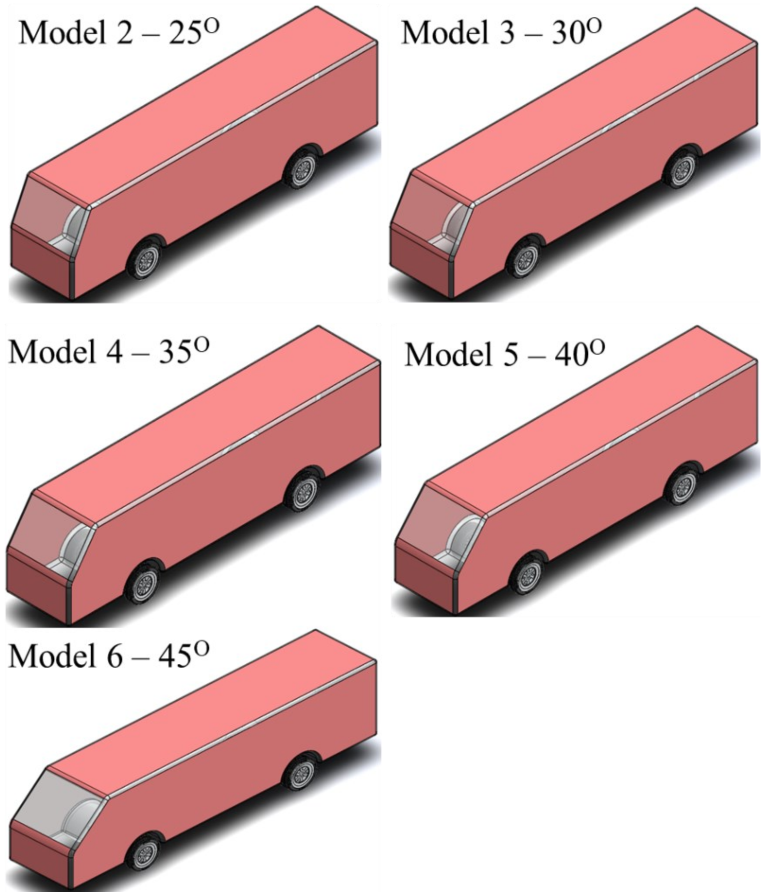

Figure 3.4: SolidWorks model assembly view of simplified new models of Anbessa bus

3.5. CFD Analysis of Anbessa Bus

There are various tools that can be utilized for CFD analysis. Here, Phoenics software is used for the CFD analysis of various models of Anbessa bus. This is done by creating fluid flow model for each of the model created by SolidWorks software. By following five basic steps, as shown in *Figure 3.5*. The whole analysis is done for both the current model and the new modified models as follows.

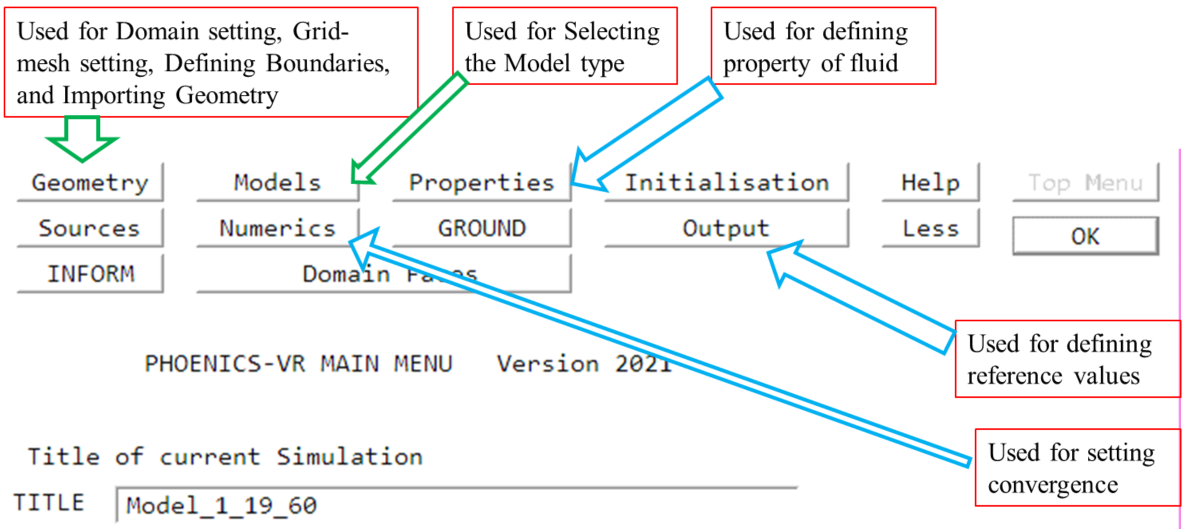

Figure 3.5: Basic procedures in Phoenics software

As shown in the *Figure 3.5*, the first step is concerned with geometry. Here, this menu consists of various substeps to be followed. These are, creating the main domain for the fluid, defining grid mesh settings, creating and defining boundaries, and importing or creating the solid model geometry. Hence, each substeps followed are discussed below.

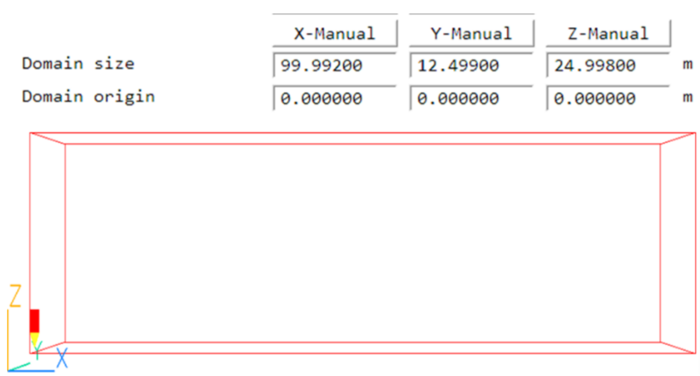

Figure 3.6: Domain settings for fluid in Phoenics software

The fluid domain is created based on the dimensions follow the criteria of Ahmed Car Body given in *Table 3.4*. as such, the fluid domain is created as shown in *Figure 3.6*.

Table 3.4: Criteria for the dimensions of Fluid domain (Christopher, 2015)

S.No.	Parameter	Criteria	Dimension
1	Length (m)	8L	8*12.499 = 99.992
2	Width (m)	L	12.499
3	Height (m)	2L	2*12.499 = 24.998

Moreover, since boundary conditions are required for the analysis, various boundarioes are created as discussed below. The first boundary created is the fluid inlet. This is done by defining the size of the inlet and the place where this inlet is located. In addition, the attribute of the inlet is defined to indicate the velocity and intensity of the fluid. Since the Anbessa bus usually works in a city its speed is usually below 60 Km/h. Thus, the simulation is developed for 60 Km/h or 16.667 m/s.

In addition, the boundary condition is created for the fluid outlet. This is done by defining the size of the outlet and the place where this oulet is located. The outlet of the fluid attributes and properties are unknown. That is, the outlet is not restricted. Thus, attributes are not for the outlet of the fluid. Then, the software determines the flow by itslef. Moreover, the boundary condition is created for the road as a ground. This is done by defining the size of the ground and the place where this ground is located. In addition, the attribute of the inlet is defined to indicate the velocity and intensity of the fluid.

Then, the geometry of the model is imported to the software. However, the Phoenics software does not accept direct model created by the SolidWorks. Thus, before importing the model created by SolidWorks, the file format must be saved in the msl format that is suitable for Phoenics software. In addition, based on the plane the model is created on the model may be rotated and scaled down to fit in the fluid domain provided. Moreover, the location of the model should be defined so that the model should be placed in the appropriate place.

Then, the grid mesh settings are defined to improve the convergence of the analysis. These is done by changing the default auto meshing into manual meshing. Then, for each of the cell is the domain, the meshing in x, y, and z is applied to the domain. In addition, the probe location is set to obtain the smooth flow transformation behind the geometry of the model.

Moreover, the number of the iteration the model run is set to 1000 iterations. Furthermore, global convergence criterion is set to 0.001%. Then, the turbulence model for the analysis is selected to be the default model the software provided. Thus Chem-Kin KE is selected for turbulence model. It is an enhancement of the standard k-ε model used in computational fluid dynamics (CFD) simulations to describe turbulent flow conditions. It improves the dynamic response of the ε equation by introducing an additional time scale (k/PK), where PK represents the volumetric production rate of k.

Then, the reference parameters are set in the output parameters of the Phoenics software. These include the reference density, reference velocity, and reference areas in x, y, and z directions, moreover, the analysis is set to calculate the drag coefficient and the drag forces in the x, y, and z directions. Finally, the analysis is set to run in the solver module of the Phoenics software.

CHAPTER FOUR

4. RESULT AND DISCUSSION

With the purpose of improving fuel economy, various windshield angle of Anbessa intercity bus is investigated and CFD analysis of the effects of windshield angle on the aerodynamics of the vehicle is performed. As such the current model has a windshield angle of 19^{O}. Whereas, 25^{O}, 30^{O}, 35^{O}, 40^{O}, and 45^{O} windshield angle are considered for the modification of windshield angle of Anbessa bus. Hence, the results obtained both from conceptual design, FEA, and optimization are discussed below.

4.1. CFD Analysis

The Phoenics software gives the result of the drag coefficient and drag force, given in in *Table 4.1,* directly along the frontal plane of the yz plane or x face of the model. Similarly, the lift force and lift coefficient can be taken as the force and coefficient along the xy plane or z face of the model or after the lift force is obtained, the lift coefficient given in *Table 4.1*, is obtained by *Equation 4.1*.

Equation 4.1

$$C_L = \frac{F_L}{0.5\rho A_f v^2}$$

Where,

- C_l is the lift coefficient,
- F_L is the lift force (N),
- ρ is the density of the fluid,
- A_f is the frontal area (m^2), and
- v is the velocity of the fluid (m/s).

Table 4.1: Performance of various model of Anbessa bus at velocity of 60 Km/h

S.No.	Model	Drag Coefficient	Drag Force (N)	Lift Coefficient	Lift Force (N)
1	Model 1 – 19^{O}	0.7067	1063.55	-0.05514	-290.22
2	Model 2 – 25^{O}	0.5870	883.50	-0.05698	-299.91
3	Model 3 – 30^{O}	0.5695	857.11	-0.04783	-251.74
4	Model 4 – 35^{O}	0.5495	827.02	-0.05351	-281.65
5	Model 5 – 40^{O}	0.5228	786.92	-0.06952	-365.89
6	Model 6 – 45^{O}	0.4933	767.12	0.57097	3005.11

As shown in *Table 4.1*, as windshield angle increases, the drag coefficient decreases. Model 1 of the bus which has lowest windshield angle of 19^{O}, has the highest drag coefficient of 0.7067. Whereas, model 6 of the bus which has highest windshield angle of 45^{O}, has the lowest drag coefficient of 0.4933. Similarly, as windshield angle increases, the drag force decreases. Model 1 of the bus which has lowest windshield angle of 19^{O}, has the highest drag force of 1063.55. Whereas, model 6 of the bus which has highest windshield angle of 45^{O}, has the lowest drag force of 767.12.

In addition, as shown in *Table 4.1,* as windshield angle increases, the lift coefficient decreases then increases then decreases and finally increases. Thus, the windshield angle has no direct relation with the lift coefficient. As such, Model 5 of the bus has the lowest lift coefficient of -0.06952. Whereas, model 6 of the bus which has highest windshield angle of 45^{O}, has the highest lift coefficient of 0.57097. Similarly, as windshield angle increases, the lift force decreases then increases then decreases and finally increases. Thus, the windshield angle has no direct relation with the lift force. As such, Model 5 of the bus has the lowest lift force of -365.89. Whereas, model 6 of the bus which has highest windshield angle of 45^{O}, has the highest lift force of 3005.11.

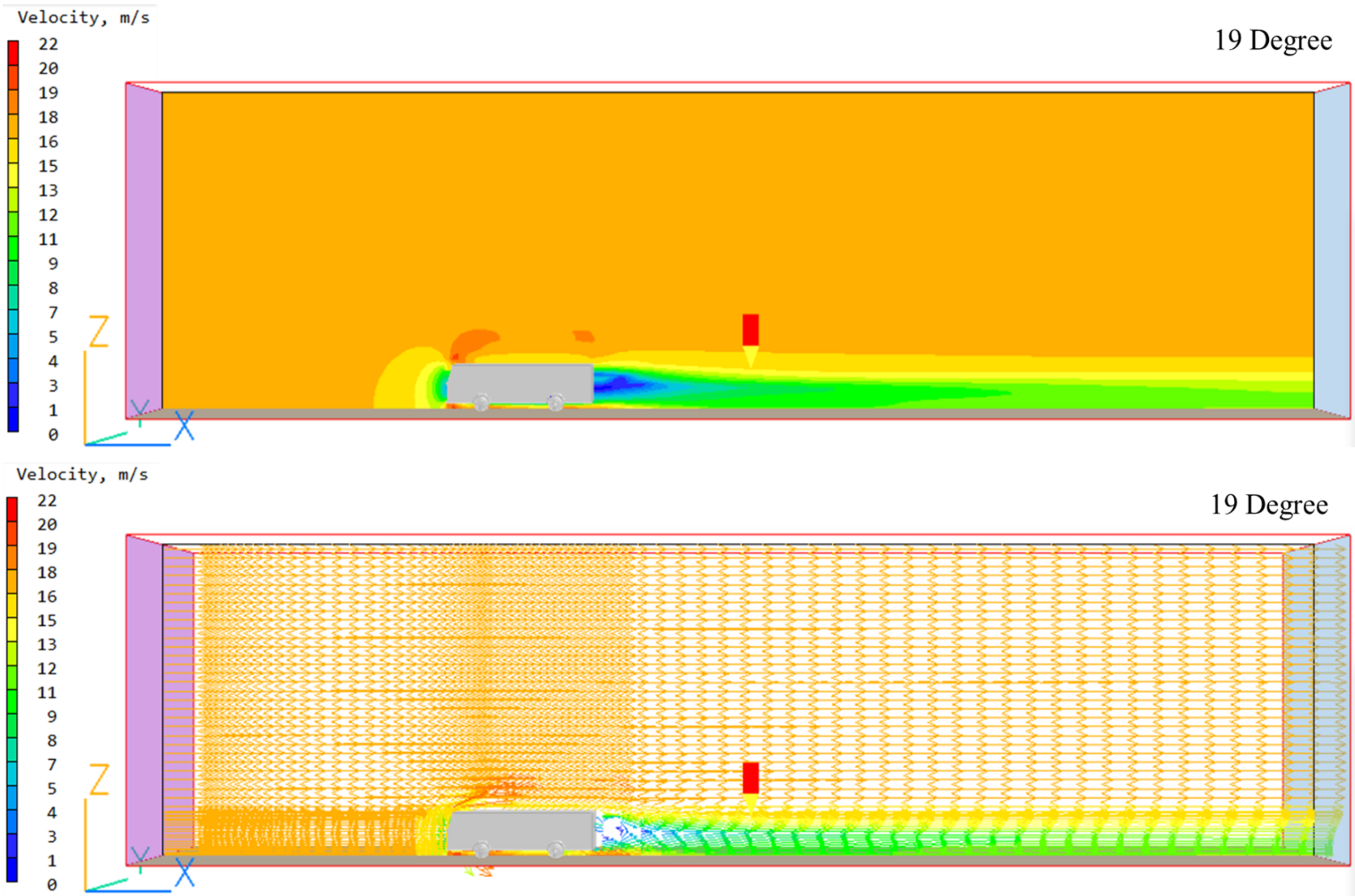

Figure 4.1: Velocity contour and Vector plot for 19^{O} Model bus in Phoenics Post Processor

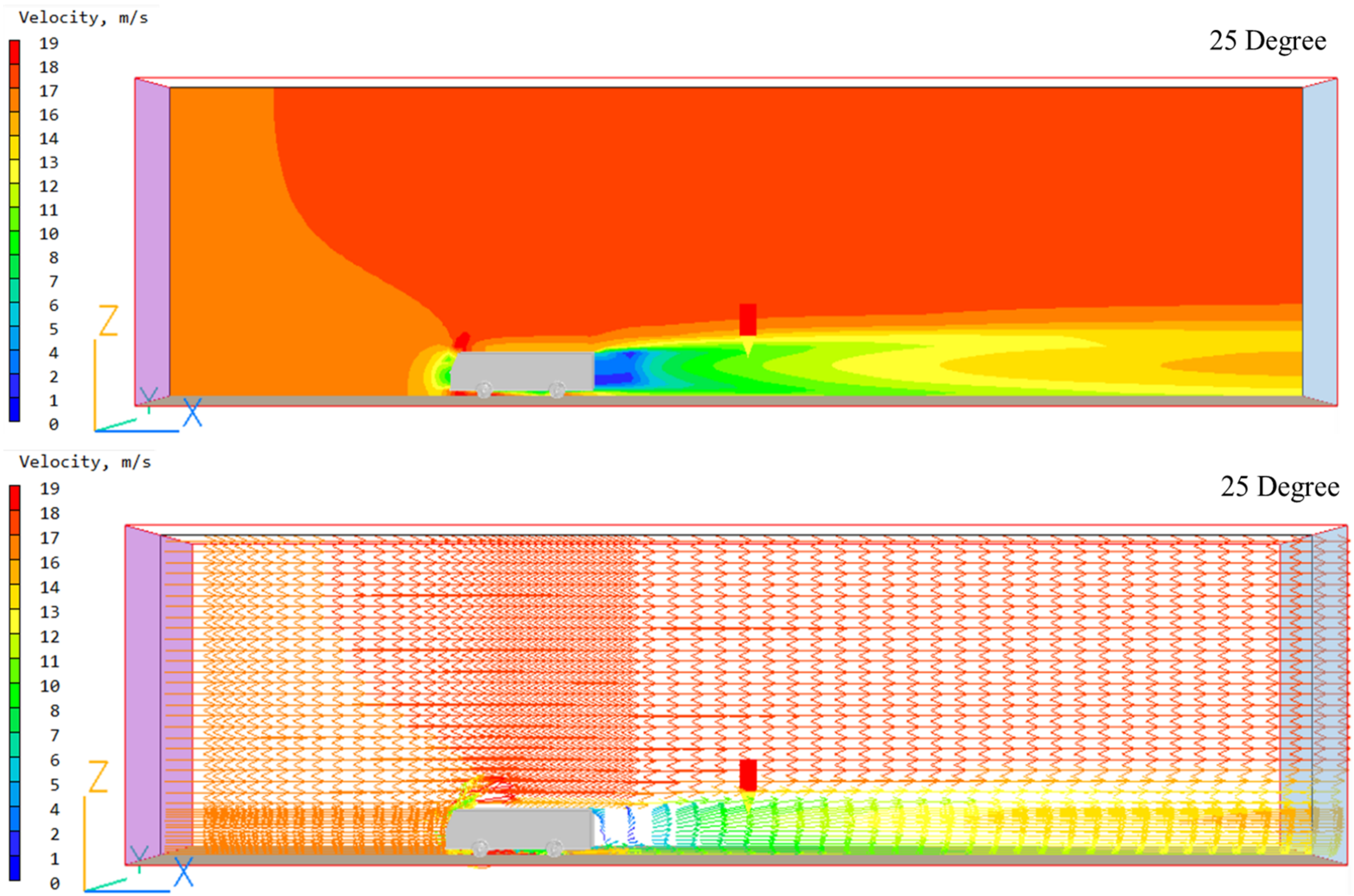

Figure 4.2: Velocity contour and Vector plot for 25^{O} Model bus in Phoenics Post Processor

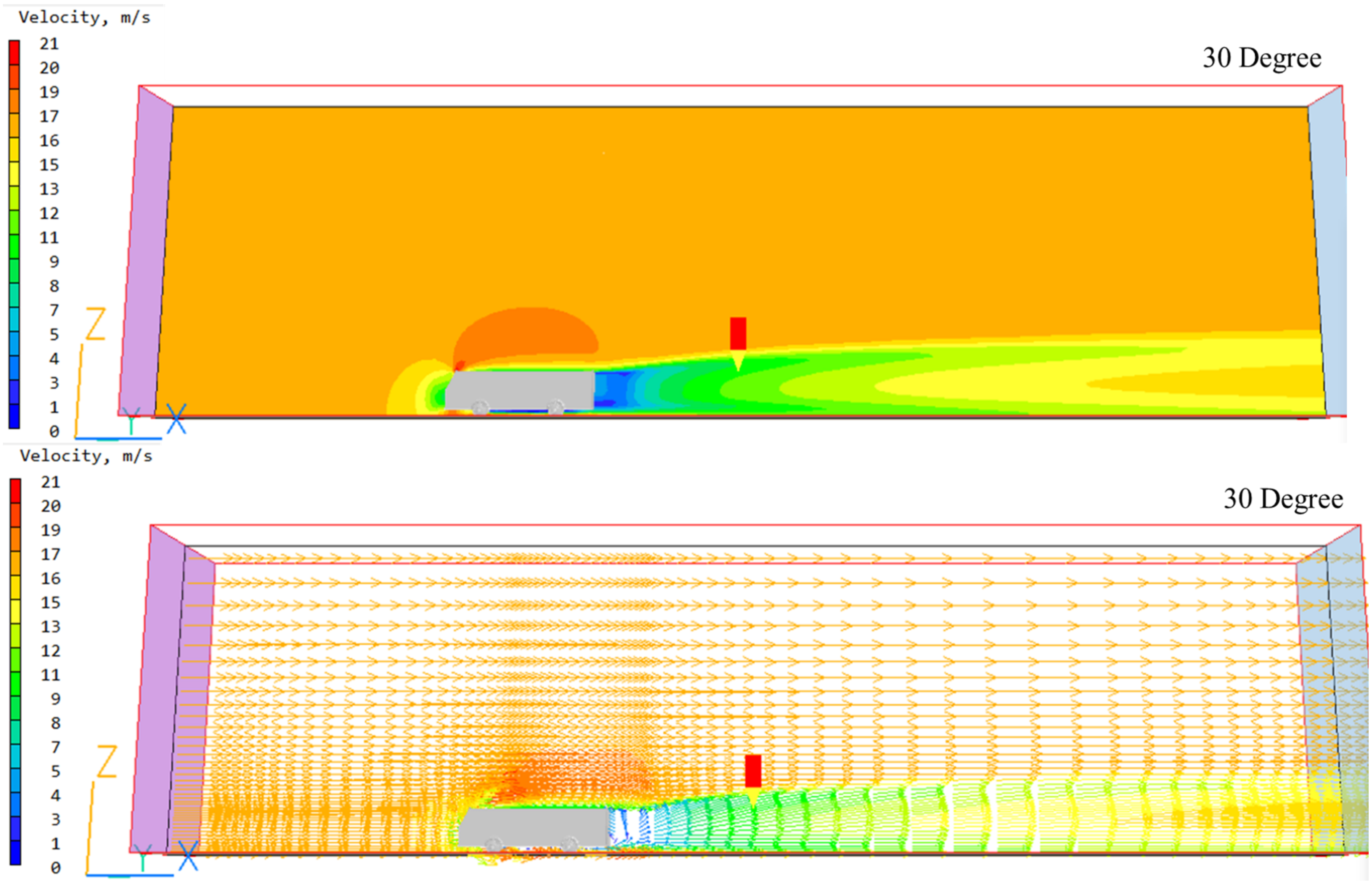

Figure 4.3: Velocity contour and Vector plot for 30^O Model bus in Phoenics Post Processor

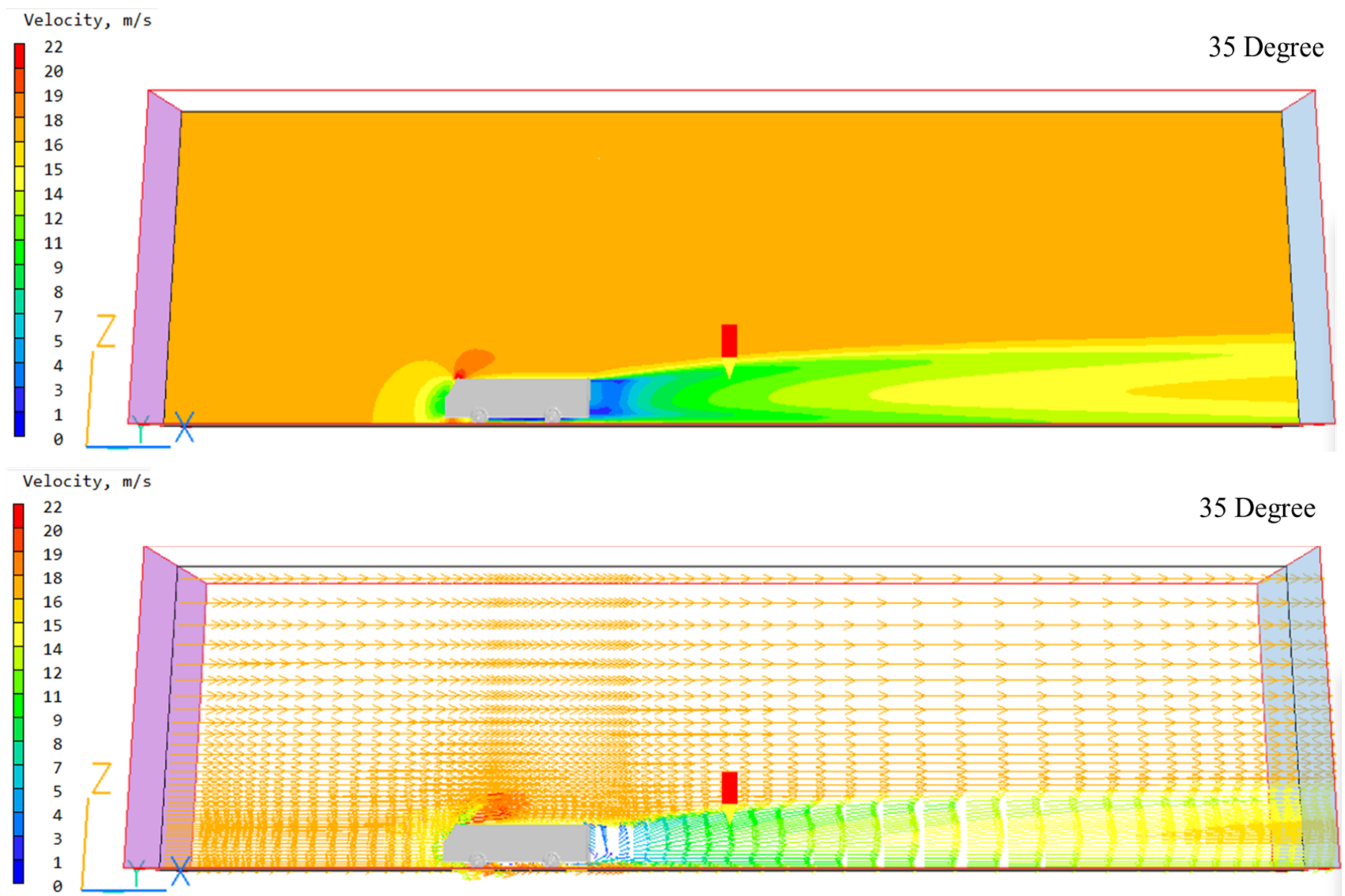

Figure 4.4: Velocity contour and Vector plot for 35^{O} Model bus in Phoenics Post Processor

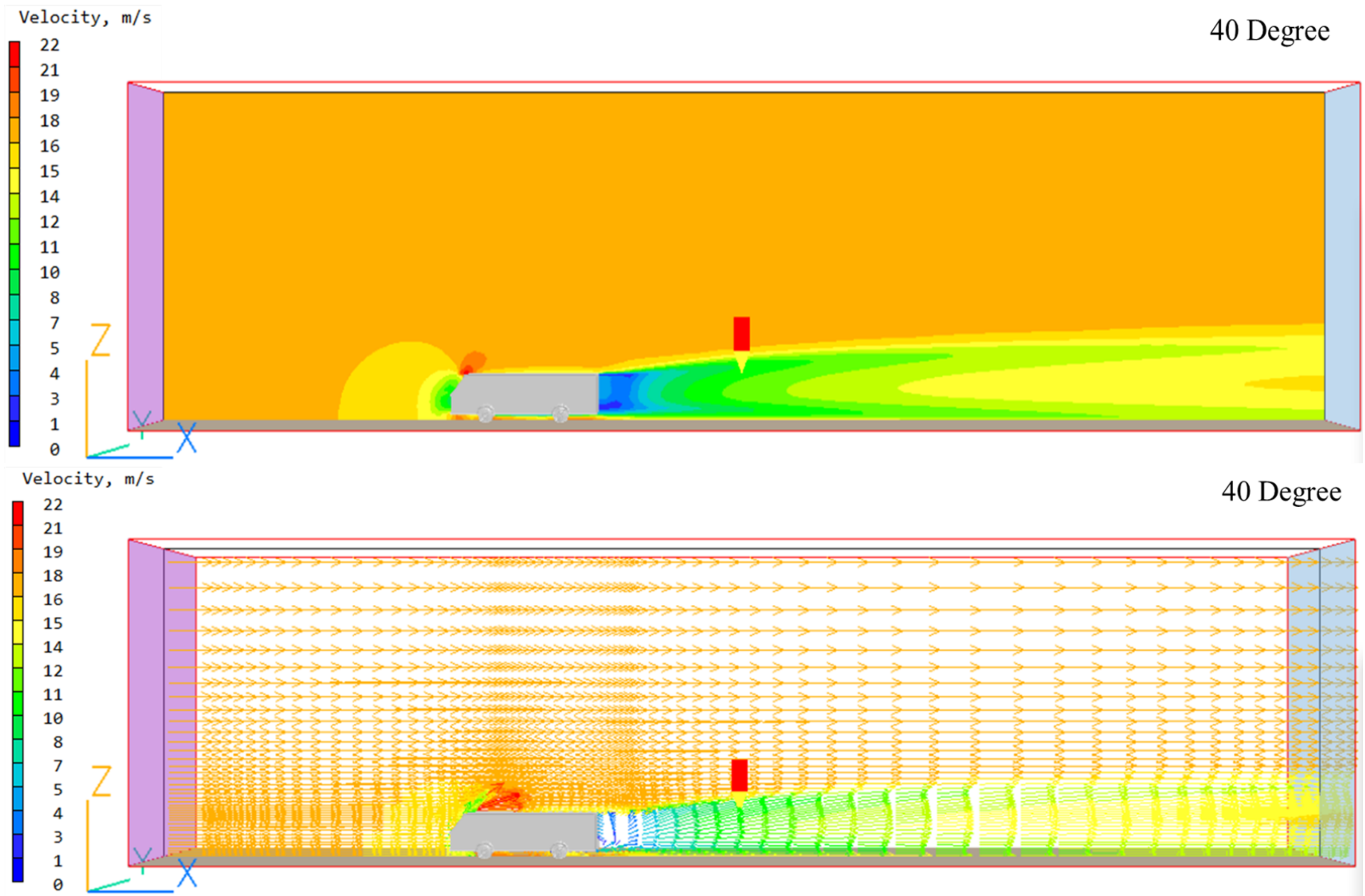

Figure 4.5: Velocity contour and Vector plot for 40^{O} Model bus in Phoenics Post Processor

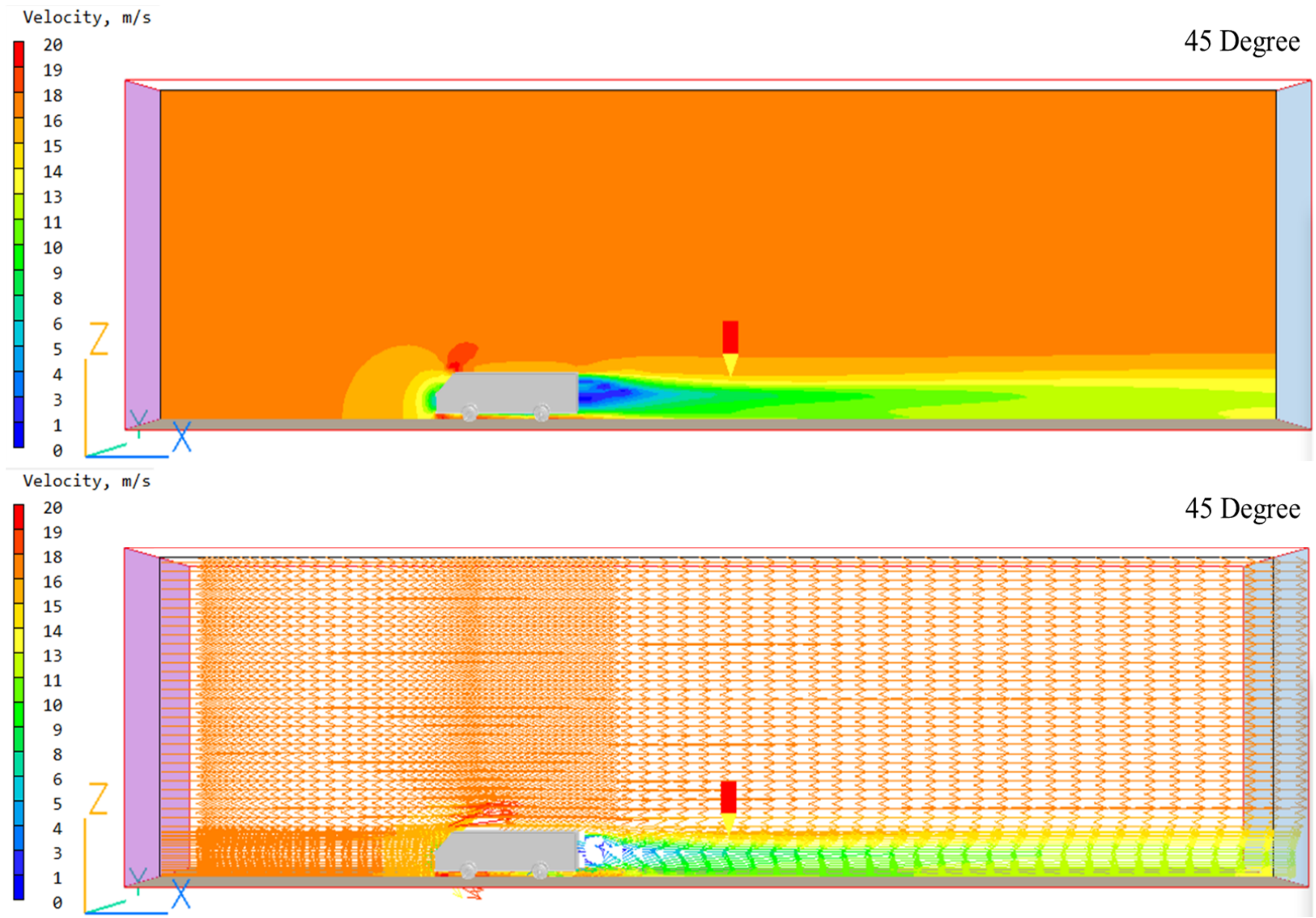

Figure 4.6: Velocity contour and Vector plot for 45^{O} Model bus in Phoenics Post Processor

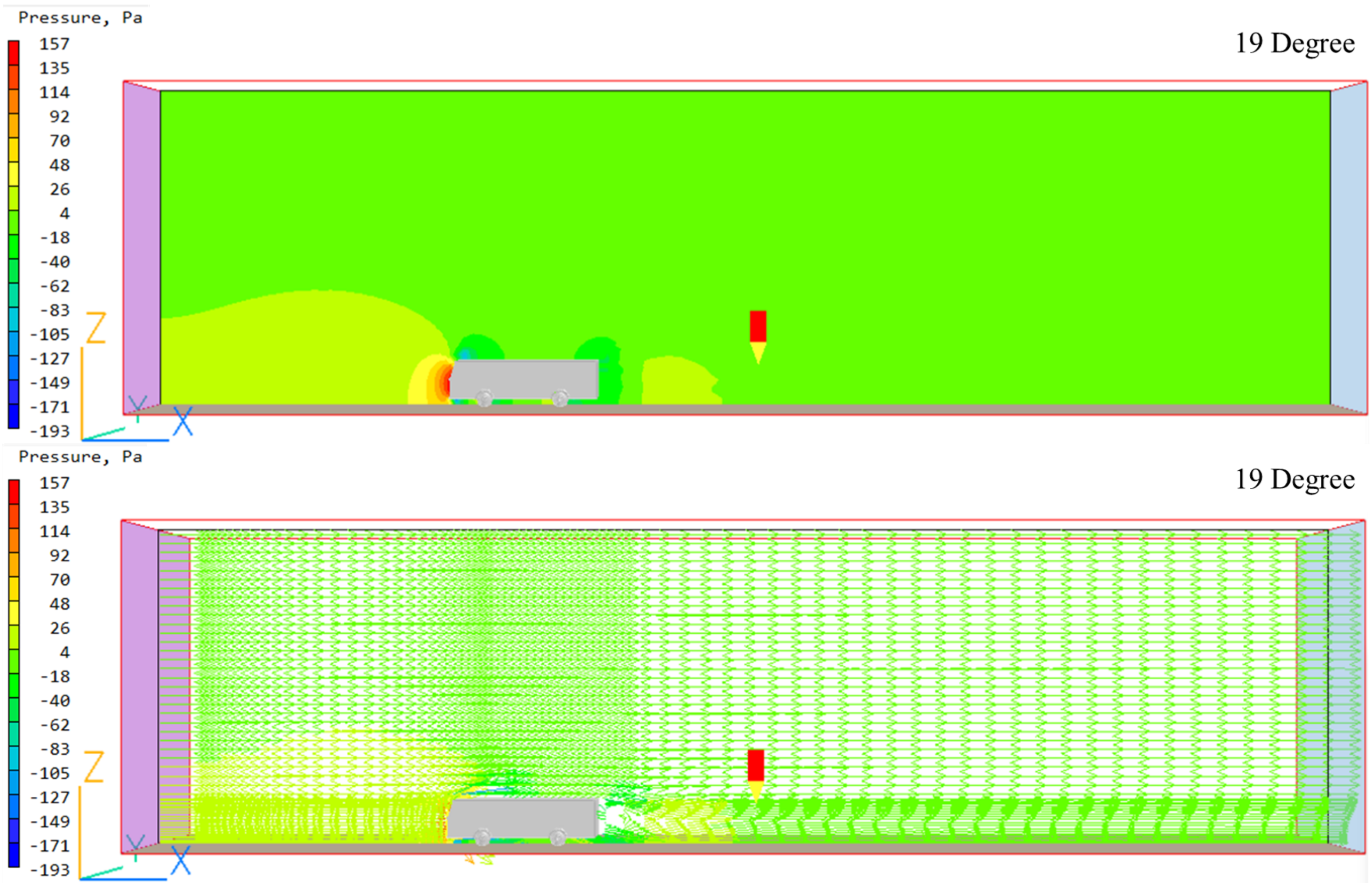

Figure 4.7: Pressure contour and Vector plot for 19^{O} Model bus in Phoenics Post Processor

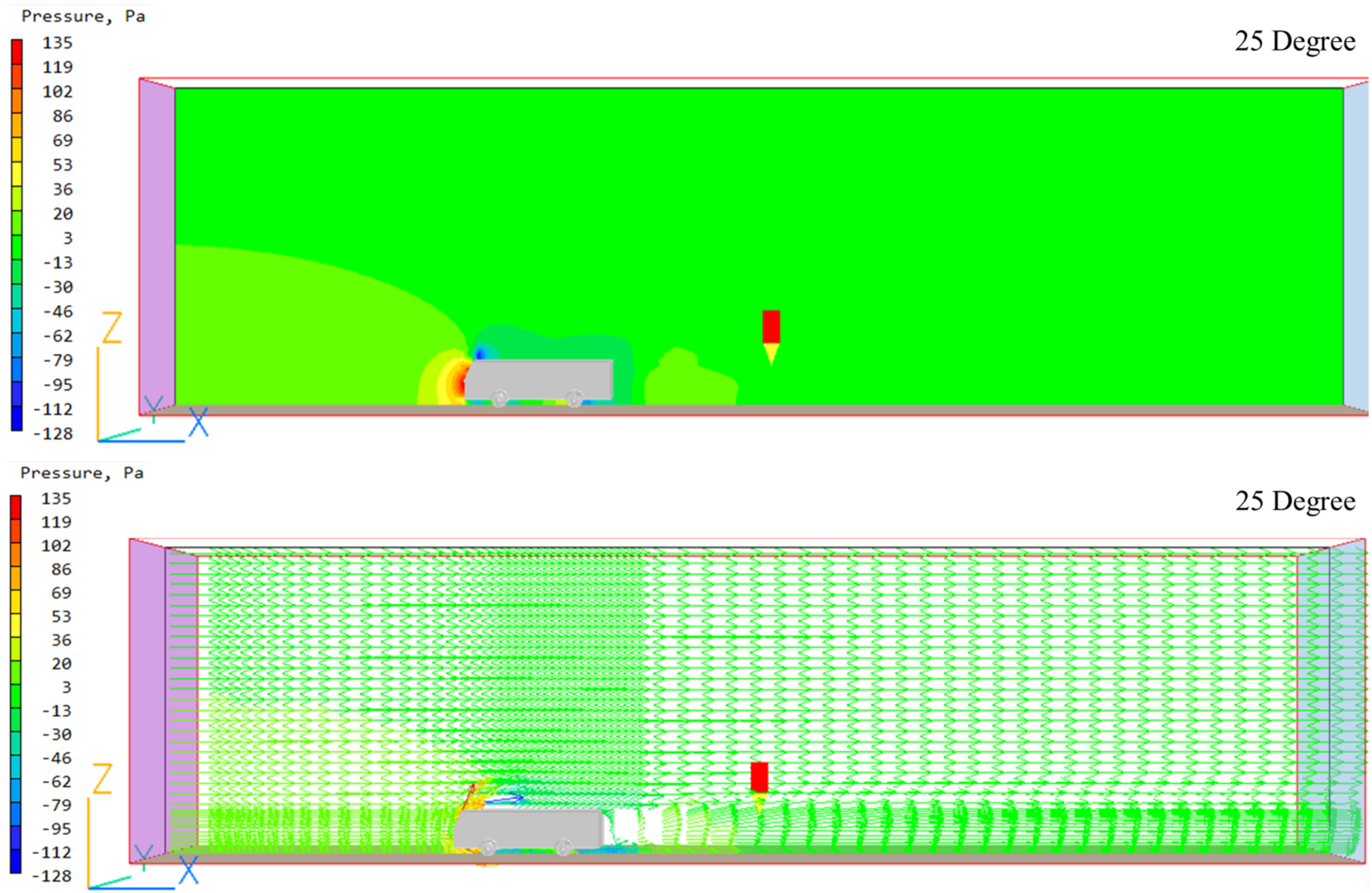

Figure 4.8: Pressure contour and Vector plot for 25^{O} Model bus in Phoenics Post Processor

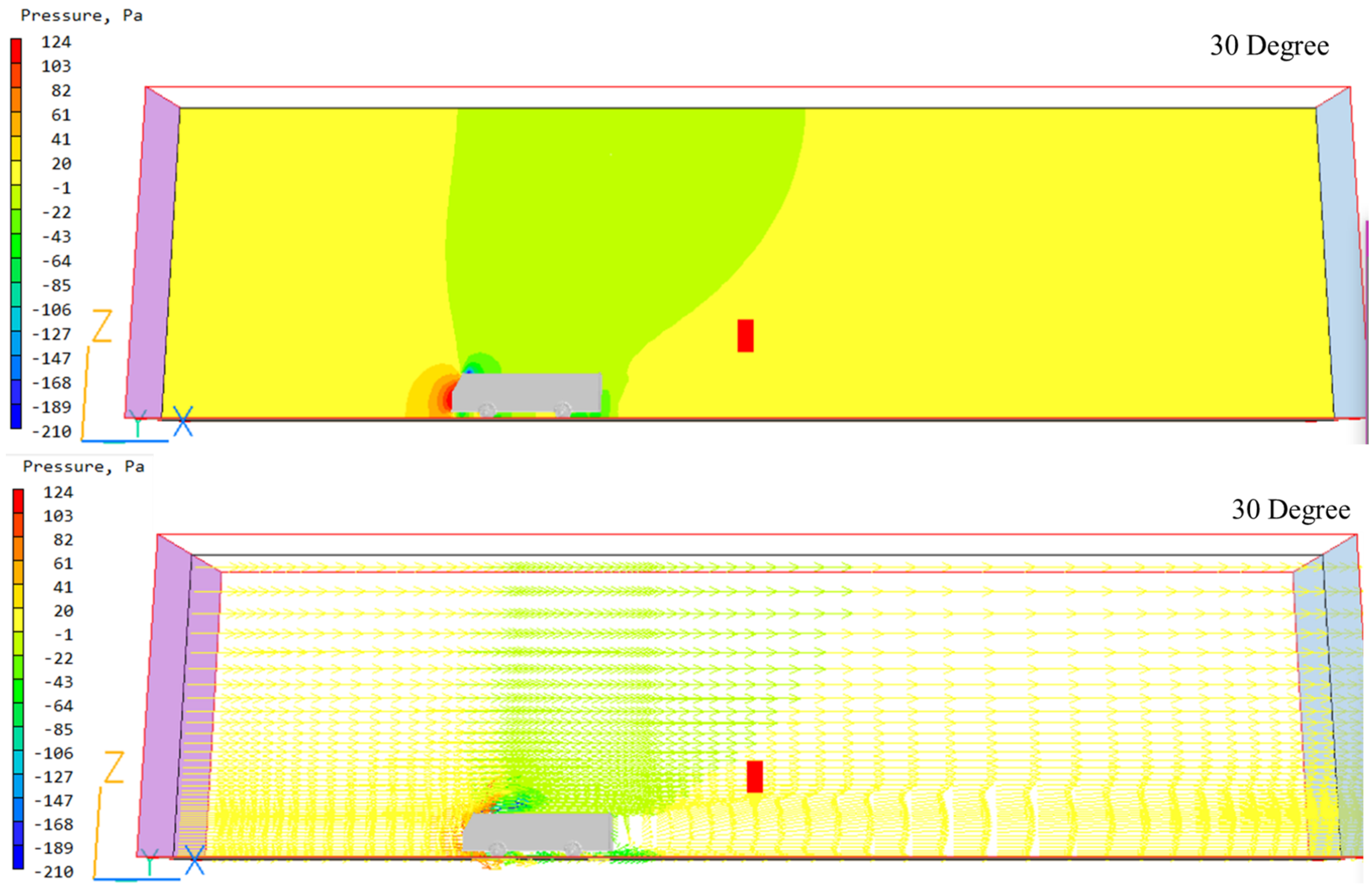

Figure 4.9: Pressure contour and Vector plot for 30^{O} Model bus in Phoenics Post Processor

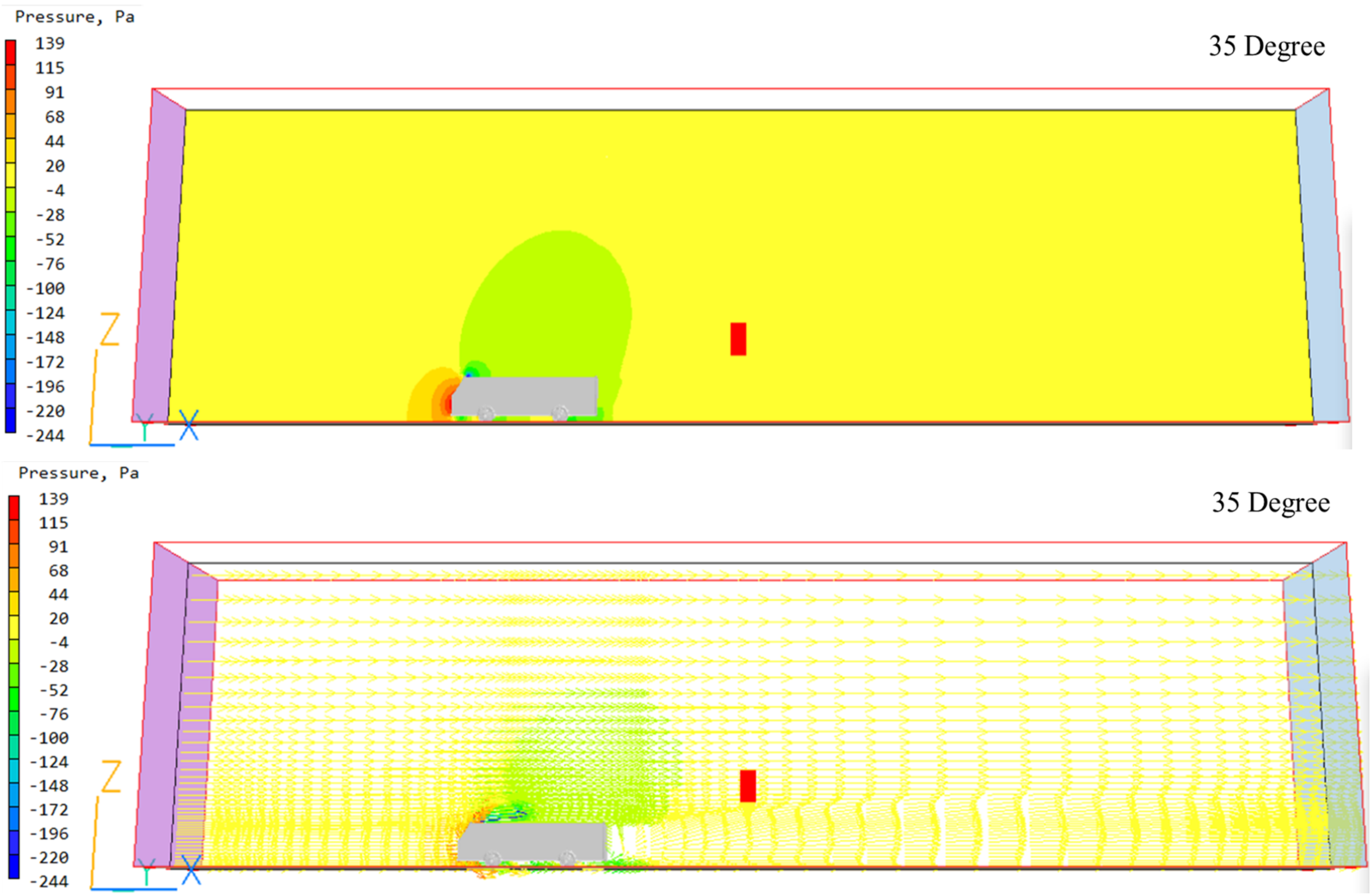

Figure 4.10: Pressure contour and Vector plot for 35^{O} Model bus in Phoenics Post Processor

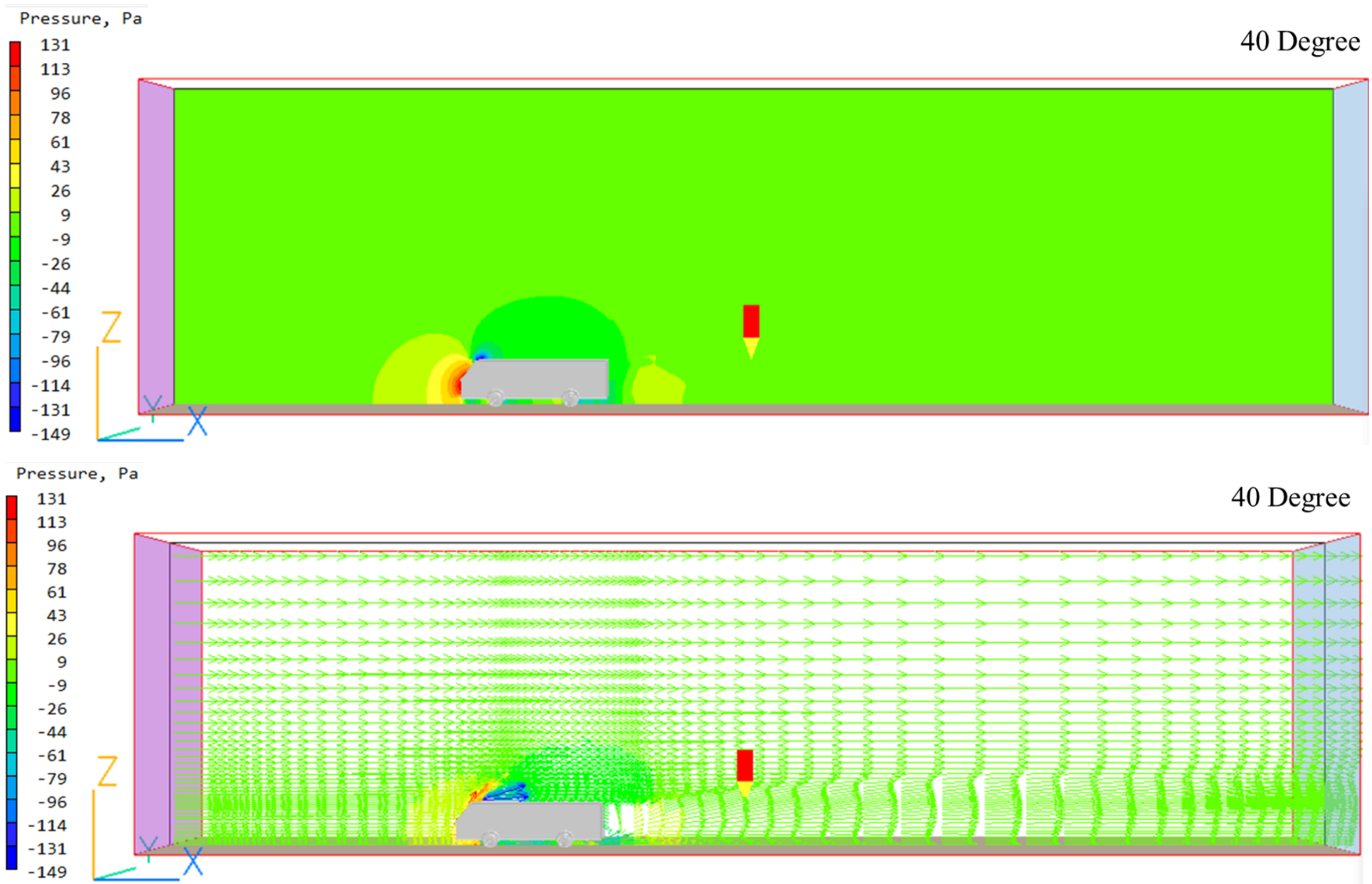

Figure 4.11: Pressure contour and Vector plot for 40^{O} Model bus in Phoenics Post Processor

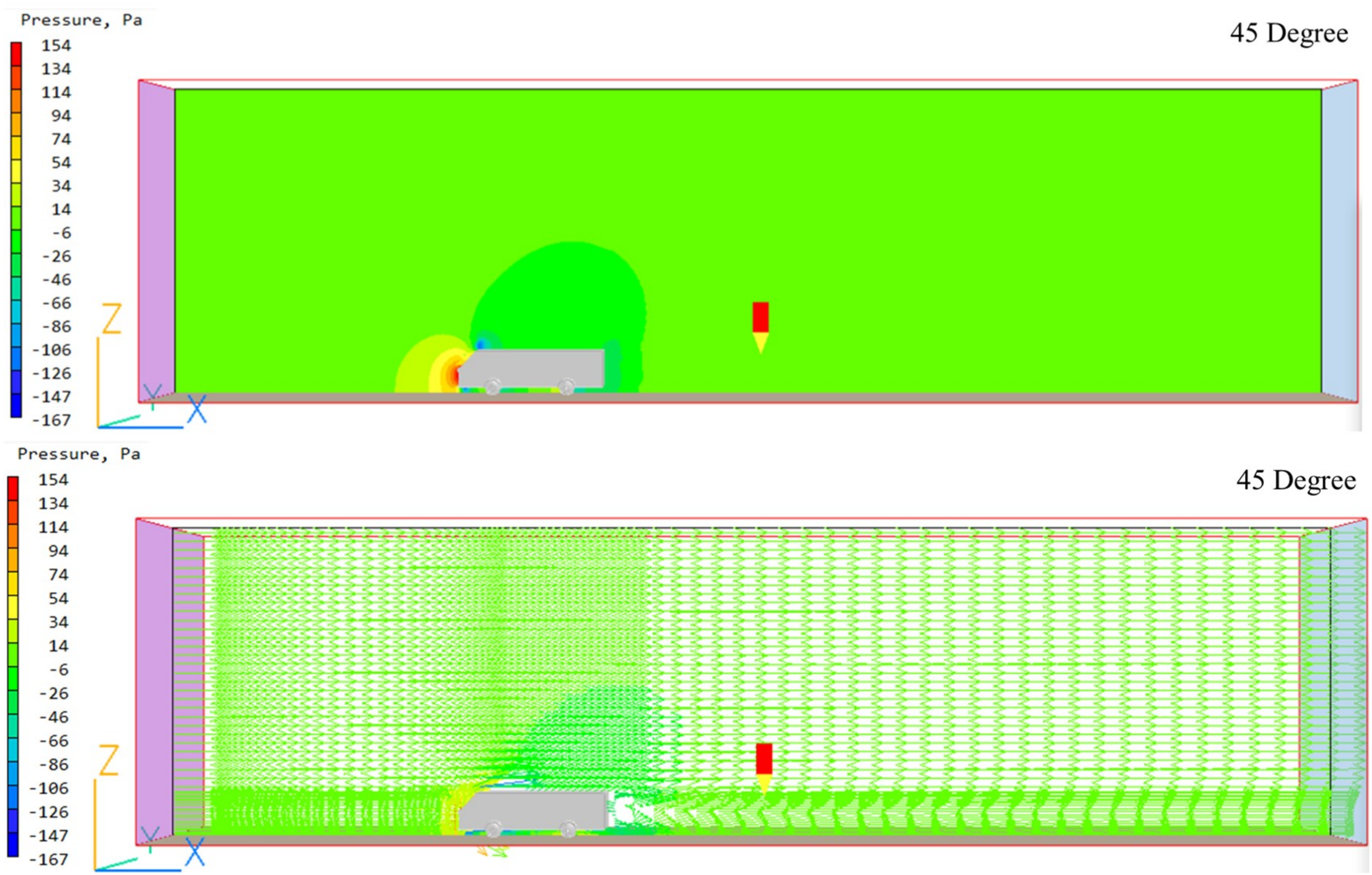

Figure 4.12: Pressure contour and Vector plot for 45^{O} Model bus in Phoenics Post Processor

Moreover, *Figure 4.1* to *Figure 4.6* shows the visualization of velocity contour on the bus surface of the current model and all the modifications of the model. The velocity contour on the bus is investigated to understand the underlying causes of the reduction of the drag force. The velocity contour of the model 1 exhibits that the bus showed the flow distribution is disturbed nearly at the beginning of the top surface of the bus. In addition, this will result in the flow separation at the rear of the bus. However, the velocity contour of the other models exhibits that, as the windshield angle increase from 19^{O} to 45^{O}, the flow become more distributed. Moreover, this will decrease the flow separation at the rear of the bus that have been witnessed in the previous model. This indicates that increase in the windshield angle is useful for distributed flow and to decrease the flow separation.

Similarly, *Figure 4.1* to *Figure 4.6* shows the visualization of velocity vector on the bus surface of the current model and all the modifications of the model. The velocity vector on the bus is investigated to understand the underlying causes of the reduction of the drag force. The velocity vector of the model 1 exhibits that the bus showed the flow distribution is disturbed nearly at the beginning of the top surface of the bus. In addition, this will result in the flow separation at the rear of the bus. However, the velocity vector of the other models exhibits that, as the windshield angle increase from 19^{O} to 45^{O}, the flow become more distributed. Moreover, this will decrease the flow separation at the rear of the bus that have been witnessed in the previous model. This indicates that increase in the windshield angle is useful for distributed flow and to decrease the flow separation.

Furthermore, *Figure 4.7* to *Figure 4.12* shows the visualization of pressure contour and pressure vector on the bus surface of the current model and all the modifications of the model. The pressure contour on the bus is investigated to understand the underlying causes of the reduction of the drag force on the vehicle. The pressure contour of the model 1 exhibits that the bus showed the pressure distribution is only focused at the front of the bus. However, the pressure contour of the other models exhibits that, as the windshield angle increase from 19^{O} to 45^{O}, the pressure become more distributed not only on the front but the other parts of the vehicle also. Furthermore, the pressure contours and vectors show that the pressure on the front vehicle decreases as the windshield angle increases.

4.2. Fuel Economy

To determine how much the fuel economy of the bus is improved, the analysis started with the determination of specific energy consumption of the base model. In addition, the fuel economy of each model is determined. Since the drag force and coefficient is determined through Phoenics simulation, the specific energy of the fuel can be determined for determining the fuel consumption of the new models. Thus, as discussed in *Equation 2.16*,

$$\phi_d = \frac{E}{F_C}$$

Where,

- F_C is the fuel consumption (L/Km),
- E is the energy consumption, and
- ϕ_d is the specific energy of the fuel (Wh/L).

As discussed in *Table 3.1*, the fuel consumption of the current Anbessa model is 4.5Km/Liter. That is, 0.222 L/Km. In addition, since the velocity of the bus and the velocity of the air are the same, the drag force can be taken as energy consumption. Hence,

$$\phi_d = \frac{1063.55}{0.222}$$

$$\boldsymbol{\phi_d = 4790.76}$$

Thus, the base model has 4790.76 Wh/L. And this can be used for all the models. Based on this the fuel consumption for all the models.

For model 2:

$$F_C = \frac{883.50}{4790.76}$$

$$\mathbf{F_C = 0.18442\,\frac{L}{Km} = 5.4224\ Km/L}$$

For model 3:

$$F_C = \frac{857.11}{4790.76}$$

$$\mathbf{F_C = 0.17891\ L/Km = 5.589\ Km/L}$$

For model 4:

$$F_C = \frac{827.02}{4790.76}$$

$$\mathbf{F_C = 0.17263\ L/Km = 5.793\ Km/L}$$

For model 5:

$$F_C = \frac{786.92}{4790.76}$$

$$\mathbf{F_C = 0.1643\ L/Km = 6.0864\ Km/L}$$

For model 6:

$$F_C = \frac{767.12}{4790.76}$$

$$\mathbf{F_C = 0.1601\ L/Km = 6.246\ Km/L}$$

Table 4.2 shows the comparison of fuel economy of various model of Anbessa bus. It indicates that, as windshield angle increases, the fuel economy of the bus increases. Model 1 of the bus which has lowest windshield angle of 19^{O}, has the lowest fuel economy of 4.5 Km/L. Whereas, model 6 of the bus which has highest windshield angle of 45^{O}, has the highest fuel economy of 6.246 Km/L.

Table 4.3 summarizes the effect of windshield angle on drag coefficient and fuel economy of Anbessa bus. It indicates that, as windshield angle increases, the drag coefficient on the bus decreases and the fuel economy of the bus increases. Model 1 of the bus which has lowest windshield angle of 19^O, has the highest drag coefficient and lowest fuel economy. Whereas, model 6 of the bus which has highest windshield angle of 45^O, has the lowest drag coefficient and highest fuel economy. Thus, by increasing the windshield angle by 26^O, the drag coefficient can be decreased by 30.20 % and the fuel economy can be improved by 38.80 %.

Table 4.2: Comparison of fuel economy of various model of Anbessa bus

S.No.	Model	Fuel economy (Km/L)	Increase in Fuel economy (%)
1	Model 1 – 19^O	4.5	-
2	Model 2 – 25^O	5.4224	20.50
3	Model 3 – 30^O	5.589	24.20
4	Model 4 – 35^O	5.793	28.73
5	Model 5 – 40^O	6.0864	35.25
6	Model 6 – 45^O	6.246	38.80

Table 4.3: Effect of windshield angle on drag coefficient and fuel economy

S.No.	Model	Drag Coefficient	Fuel economy (Km/L)	Increase in Angle (^{O})	Decrease in Drag coefficient (%)	Increase in Fuel economy (%)
1	Model 1 – 19^O	0.7067	4.5	-	-	-
2	Model 2 – 25^O	0.5870	5.4224	6	16.94	20.50
3	Model 3 – 30^O	0.5695	5.589	11	19.41	24.20
4	Model 4 – 35^O	0.5495	5.793	16	22.24	28.73
5	Model 5 – 40^O	0.5228	6.0864	21	26.02	35.25
6	Model 6 – 45^O	0.4933	6.246	26	30.20	38.80

4.3. Optimization

As shown in *Table 4.1*, as windshield angle increases, the drag coefficient decreases. Moreover, as shown in *Table 4.2*, as windshield angle increases, the fuel economy of the bus increases. Whereas, as shown in *Table 4.1*, direct relation could not be obtained for the windshield angle and lift coefficient. Furthermore, at 45^O windshield angle, the lift coefficient becomes positive. However, only negative lift coefficient is are used for land vehicles. Thus, optimizing these parameters are necessary. Thus, DESIGN EXPERT software is used to optimize these parameters. These is done by considering the windshield angle as input or factor, and drag coefficient, lift coefficient, and fuel economy as response parameters, as shown in *Table 4.4*.

Table 4.4: Factor and response parameters in DESIGN EXPERT software

Run	Factor 1 A:Windshield an...	Response 1 Drag Coefficient	Response 2 Lift Coefficient	Response 3 Fuel economy
1	19	0.7067	-0.05514	4.5
2	25	0.587	-0.05698	5.4224
3	30	0.5695	-0.04783	5.589
4	35	0.5495	-0.05351	5.793
5	40	0.5228	-0.06952	6.0864
6	45	0.4933	0.57097	6.246

Then, the software provided three regression equation based on the analysis of the variance three types of models recommended by the software. As such, linear model is used for the modeling of drag coefficient, as shown in *Equation 4.2*, to indicate the relationship between the windshield angle and drag coefficient.

$$Drag\ coefficient = 0.5739 - 0.0936A \qquad \text{Equation 4.2}$$

Where,

- ✓ A is the input factor or windshield angle.

Whereas, cubic model is used for the modeling of lift coefficient, as shown in *Equation 4.3*, to indicate the relationship between the windshield angle and lift coefficient.

$$Lift\ coefficient = -0.113 - 0.1734A + 0.3466A^2 + 0.4809A^3 \qquad \text{Equation 4.3}$$

Where,

- ✓ A is the input factor or windshield angle.

Moreover, quartic model is used the modeling of fuel economy, as shown in *Equation 4.4*, to indicate the relationship between the windshield angle and fuel economy.

$$Fuel\ Economy = 5.66 + 0.44A + 0.4396A^2 + 0.4323A^3 - 0.7231A^4 \qquad \text{Equation 4.4}$$

Where,

- ✓ A is the input factor or windshield angle.

Then, as shown in *Table 4.5*, the constraints or criteria for the optimizations are set. That is, as windshield angle increases, the drag coefficients need to be decreased, fuel economy is required to increases, and lift coefficients are required to be negative values.

Table 4.5: Setting Optimization Criteria in DESIGN EXPERT software

Name	Goal	Lower Limit	Upper Limit
A:Windshield angle	is in range	19	45
Drag Coefficient	minimize	0.4933	0.7067
Lift Coefficient	minimize	-0.06952	0
Fuel economy	maximize	4.5	6.246

Table 4.6: Solution for optimization in DESIGN EXPERT software

Number	Windshield angle	Drag Coefficient	Lift Coefficient	Fuel economy	Desirability	
1	**38.068**	**0.530**	**-0.070**	**5.967**	**0.886**	**Selected**
2	20.108	0.659	-0.032	4.784	0.256	

As such, after optimizing the parameters, the DESIGN EXPERT provided two alternative solutions, as shown in *Table 4.6*. It includes the optimized parameters for all the 3 response parameters. For both of the optimization runs, desirability factor is provided.

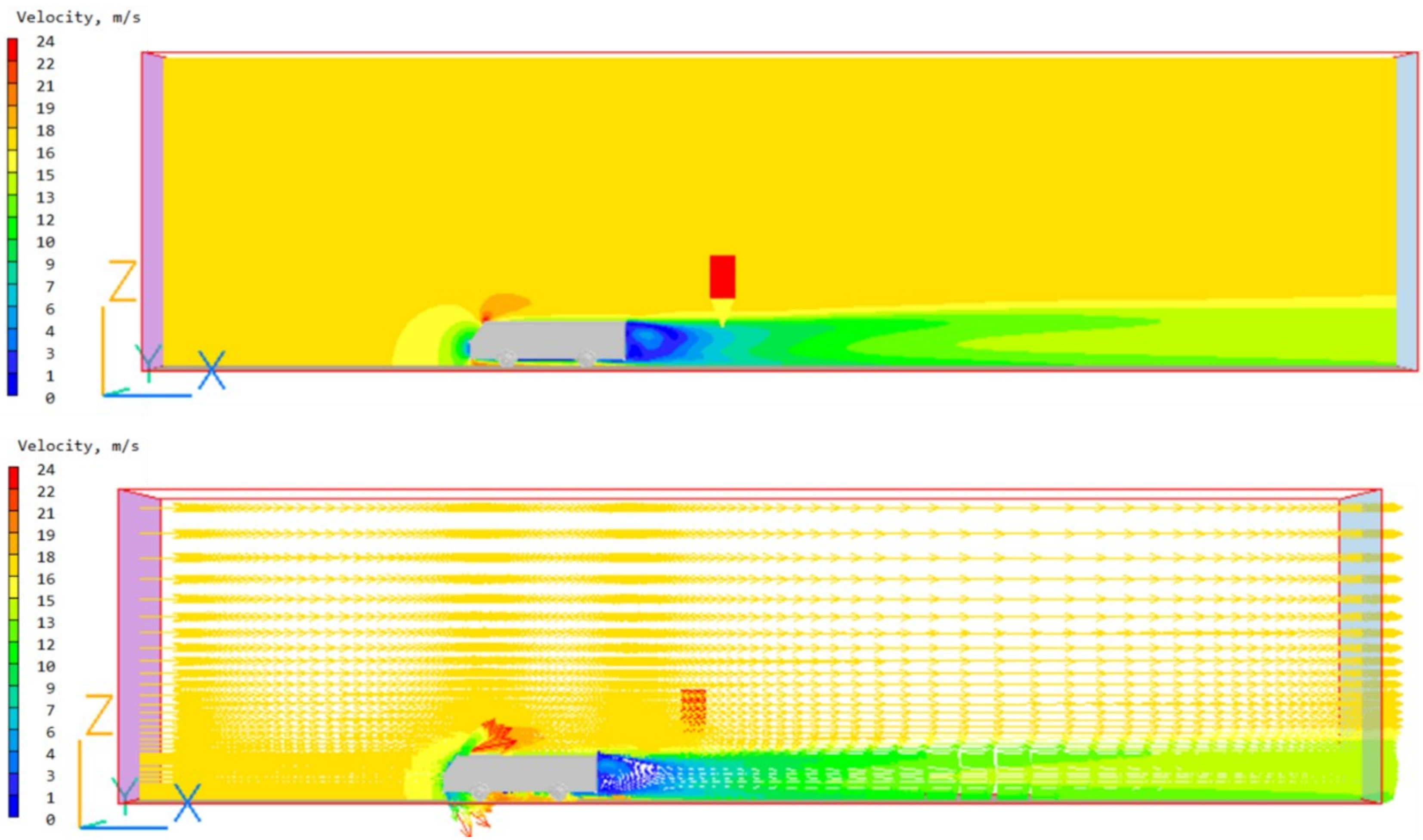

Figure 4.13: Velocity contour and vector plot of the optimized model in Phoenics

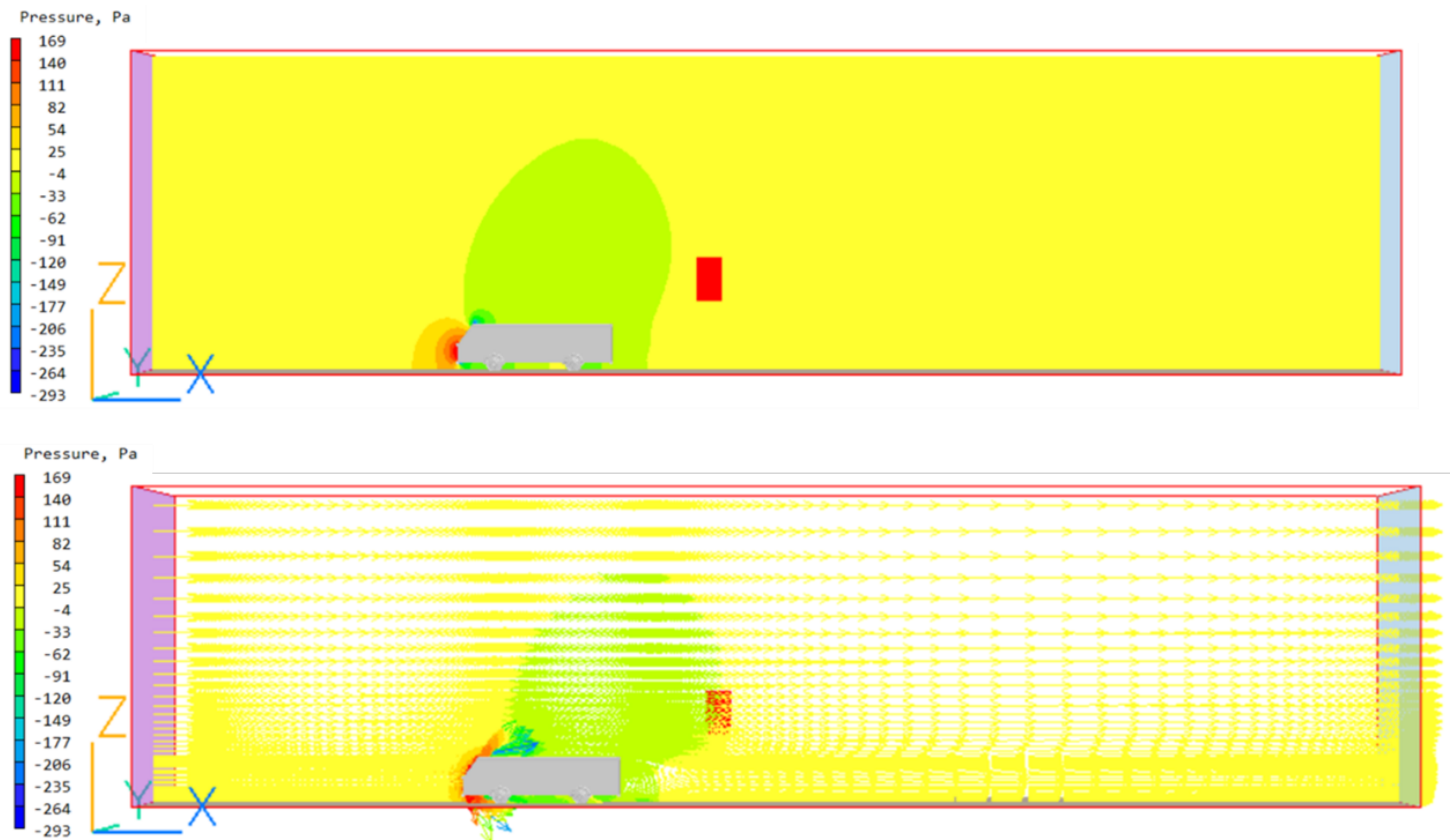

Figure 4.14: Pressure contour and vector plot of the optimized model in Phoenics

Hence, the model with desirability factor of 0.886 is selected and suggested by the software. This optimized model recommends to use a windshield angle of 38.068^{O}. At this windshield angle, drag coefficient, lift coefficient, and fuel economy are 0.53, -0.07, and 5.967, respectively. While determining these values the calculation for drag coefficient, lift coefficient, and fuel economy obtains the R^2 value of 0.8727, 0.9375, and 0.9999, respectively.

Finally, using the optimized windshield angle of 38.068^{O}, the Phoenics gives the result of drag coefficient, and lift coefficient, are 0.53, and -0.071, respectively. These results are similar to the results obtained from the DESIGN EXPERT software. In addition, as shown in *Figure 4.13*, the velocity contour and velocity vector of the optimized model exhibits that, the flow become more distributed and the flow separation at the rear of the bus is decreased. Furthermore, as shown in *Figure 4.14,* the pressure contour of the other models exhibits that, the pressure become more distributed not only on the front but the other parts of the vehicle also.

4.4. Validation

Various researchers have performed optimization of bus models to reduce drag coefficient and improve fuel economy. As such, (Damissie & Babu, 2017) have optimized Yutong cross-country bus model using CFD software FLUENT 14.5 to reduce the drag force. They obtain a considerable reduction in 39.4% drag force reduction and saved 22.8% of fuel for every 100 Km. That is 57.8% fuel consumption reduction for every drag coefficient reduction. In addition, (Bayındırlı & Çelik, 2020) obtained 0.4% drag reduction by increasing every 1 degree of windshield angle. Moreover, according to a study by the National Renewable Energy Laboratory (NREL), even a 1° reduction in windshield angle can improve fuel efficiency by up to 0.5% (Hicks, 2014). Here, in this thesis, by increasing every 1 degree of windshield angle, 1.32% drag reduction is obtained. Whereas, a 1° reduction in windshield angle improved fuel economy by up to 1.7%. The results obtained deviate from the literatures fuel economy is due to various reasons. For instance, in this thesis, latest softwares have been utilized. In addition, rather than using the traditional assumption value of 60% ratio of fuel economy to drag ratio, mathematical calculations are utilized to obtain the fuel economy.

CHAPTER FIVE

5. CONCLUSION AND RECOMMENDATION

5.1. Conclusion

Anbessa Intercity Bus has very poor external body shape, and hence has very high aerodynamic drag that significantly increases its fuel consumption as it moves. However, by reducing the windshield angle, the drag force can be minimized, resulting in improved fuel efficiency. Thus, this thesis aims to study the aerodynamic performances of the existing Anbessa Intercity Bus with special focus on the effects of the windshield angle on its fuel consumption.

The study compares six models of Anbessa bus, which are developed based on the windshield angle. As such the current model has a windshield angle of 19^{O}. Whereas, 25^{O}, 30^{O}, 35^{O}, 40^{O}, and 45^{O} windshield angle are considered for the modification of windshield angle of Anbessa bus. Model 1 of the bus which has lowest windshield angle of 19^{O}, has the highest drag coefficient of 0.7067. Whereas, model 6 of the bus which has highest windshield angle of 45^{O}, has the lowest drag coefficient of 0.4933. In addition, model 1 of the bus which has lowest windshield angle of 19^{O}, has the highest drag force of 1063.55. Whereas, model 6 of the bus which has highest windshield angle of 45^{O}, has the lowest drag force of 767.12.

Moreover, the flow distribution of model 1 is disturbed nearly at the beginning of the top surface of the bus, and the flow separation occur at the rear of the bus. However, as the windshield angle increase from 19^{O} to 45^{O}, the flow become more distributed, and the flow separation at the rear of the bus decreased that have been witnessed in the previous model.

Furthermore, the pressure distribution of model 1 is only focused at the front of the bus. However, as the windshield angle increase from 19^{O} to 45^{O}, the pressure become more distributed not only on the front but the other parts of the vehicle also. And, the pressure on the front vehicle decreases as the windshield angle decreases. In addition, model 1 of the bus which has lowest windshield angle of 19^{O}, has the lowest fuel economy of 4.5 Km/L. Whereas, model 6 of the bus which has highest windshield angle of 45^{O}, has the highest fuel economy of 6.246 Km/L. That is, as windshield angle increases, the fuel economy of the bus increases.

Then, DESIGN EXPERT software is used to optimize the windshield angle that reduces drag coefficient, increase fuel economy and make sure that lift coefficient is set to negative at all-time. As such, the optimized model with desirability factor of 0.886 is selected to give a windshield angle of 38.068^{O}. At this windshield angle, drag coefficient, lift coefficient, and fuel economy are 0.53, -0.07, and 5.967, respectively. While determining these values the calculation for drag coefficient, lift coefficient, and fuel economy obtains the R^2 value of 0.8727, 0.9375, and 0.9999, respectively.

Finally, it can be concluded that:

- As windshield angle increases, the drag coefficient on the bus decreases and the fuel economy of the bus increases.
- Model 1 of the bus which has lowest windshield angle of 19^{O}, has the highest drag coefficient and lowest fuel economy.
- The optimized model of the bus which has highest windshield angle of 38.068^{O}, has the lowest drag coefficient and highest fuel economy.
- By increasing windshield angle by 19.1^{O}, fuel economy can be improved by 32.6 %.

5.2. Recommendation

CFD analysis of the effects of windshield angle on fuel economy and optimization for the locally assembled Anbessa intercity bus is performed. Six models are developed and their drag coefficient and fuel economy are compared. Moreover, the optimization is performed by considering drag, lift, and fuel economy. However, the models may need to be further analyzed for accessibility and appearance. Furthermore, the models may need be further modeled for streamline by adding curves and fillets. Thus, it is recommended that:

- The models may need to be further streamlined by adding curves and fillets on the edge of the models.

REFERENCES

Abdellah, E., & Bo, W. (2017). CFD analysis on effect of front windshield angle on aerodynamic drag. *IOP Conf. Series: Materials Science and Engineering*. https://doi.org/10.1088/1757-899X/231/1/012173

ACADS-BSG. (2024). *Phoenics*. Computational Fluid Dynamics. https://www.acadsbsg.com.au/phoenics/

Ahmed, H., & Chacko, S. (2012). Computational Optimization of Vehicle Aerodynamics. *Annals & Proceedings of DAAAM International*, *23*(1), 313–318.

Ali, Y., Joty, S. M., & Inam, M. I. (2017). Design optimization & Numerical analysis of different bus geometry to reduce air drag co-efficient and fuel consumption. *International Conference on Mechanical, Industrial and Materials Engineering*, 28–30.

Anbassa City Bus Service Enterprise. (2014). *Addis Ababa city buses*.

Anderson, J. D. (2011). *Fundamentals of Aerodynamics* (Fifth Edit). McGraw Hill Series in Aeronautical and Aerospace Engineering.

Arteaga, O., Morales, H., Terán, H., Chacon, S., Lara, M. A., Rocha-Hoyos, J., Argüello, É., & Aguirre, R. P. (2020). Aerodynamic optimization of the body of a bus. *IOP Conf. Series: Materials Science and Engineering*. https://doi.org/10.1088/1757-899X/872/1/012002

Bayindirli, C., & Celik, M. (2022). Experimental Optimization of Aerodynamic Drag Coefficient of a Minibus Model with Non-smooth Surface Plate Application. *Journal of Engineering Studies and Research*, *28*(4), 34–40.

Bayındırlı, C., & Çelik, M. (2020). The determination of effect of windshield ınclination angle on drag coefficient of a bus model by CFD method. *International Journal of Automotive Engineering and Technologies*, *9*(3), 122–129.

Bechtold, R. L., & Regency, H. (2018). Ingredients of Fuel Economy. *SAE TECHNICAL*

PAPER SERIES.

Berry, I. M. (2010). *The Effects of Driving Style and Vehicle Performance on the Real-World Fuel Consumption of U.S. Light-Duty Vehicles*. Massachusetts Institute of Technology.

Cakir, M. (2012). *CFD study on aerodynamic effects of a rear wing / spoiler on a passenger vehicle*. Santa Clara University.

Capitol Technology University. (2019). *What is SOLIDWORKS?*

Cengel, Y. A., & Cimbala, J. M. (2006). *Fluid Mechanics - Fundamentals and Applications*. McGraw Hill Series in Mechanical Engineering.

CFD Flow Engineering. (2023). *CFD Modeling of Vehicle Aerodynamics*.

Christopher, B. (2015). *Studying the Airflow Over a Car Using an Ahmed Body*. COMSOL. https://www.comsol.com/blogs/studying-the-airflow-over-a-car-using-an-ahmed-body/

Damissie, H. Y., & Babu, N. R. (2017). Aerodynamic Drag Reduction on Locally Built Bus Body using Computational Fluid Dynamics (CFD): A Case Study at Bishoftu Automotive Industry. *International Journal of Engineering Research & Technology*, *6*(11), 276–283.

Elrawemi, M., & Aburawey, I. (2019). The effect of front and rear windscreen angles on the aerodynamic drag force of a simplified car model. *International Journal of Energy Applications and Technologies*, *6*(3), 83–88. https://doi.org/10.31593/ijeat.610436

Ethio Engineering group. (2023). *YUTONG Bus Model ZK6126HGA - Bishoftu Automotive manufacturing industry*.

Ghurri, A., Alim, M., Nara, M., Adi, P., Galang, S., Putra, B., Mantik, E., Suharto, S., & Anderson, R. (2023). CFD Simulation of Aerodynamics Truck Using Cylinder as Drag Reduction Device. *Journal of Advanced Research in Fluid Mechanics and Thermal Sciences*, *2*(2), 166–181.

Goney, A. (2017). Computational Analysis of Drag Forces on Car Profiles. *International*

Journal for Research in Applied Science & Engineering Technology, *5*(Xi), 1769–1775.

Hai-tao, B. (2012). Study of different rear windscreen Angles on passenger car characteristic. *The 7th International Conference on Computer Science & Education*.

He, Z., Qu, X., Ji, L., Wu, W., & Wang, X. (2020). Analysis and Optimization of Truck Windshield Defroster. *Applied Sciences*, *10*.

Hicks, M. (2014). Summary of Fuel Economy Performance. *U.S. Department of Transportation*.

Howell, J., Windsor, S., & Passmore, M. (2021). Some Observations on Shape Factors Influencing Aerodynamic Lift on Passenger Cars. *Fluids*, *6*(44).

Hui, Z., Hao, Y., & Zhigang, Y. (2020). *Numerical Analysis on Effect of Back/Front Windshield and Hood angle on Automotive Aerodynamic Drag*.

Jeyasingham, S., & Zhu, X. (2018). Vehicle Exterior Aerodynamic Development Using Design of Experiments (DOE). *SAE Technical Paper Series*.

JingFu, H. (2023). *Yutong ZK6126HGA City Bus Details*. Bus Coach.

Juhala, M. (2014). Improving vehicle rolling resistance and aerodynamics. *Alternative Fuels and Advanced Vehicle Technologies*, 462–475. https://doi.org/10.1533/9780857097422.2.462

Karthik, K. (2015). *Vehicular Aerodynamics*. New Emerging Automobile Technologies.

Korkut, T. B., & Gören, A. (2020). Aerodynamic Effect of Wing Mirror Usage on the Solaris 7 Solar Car and Demobil 09 Electric Vehicle. *International Journal of Automotive and Mechanical Engineering*, *17*(1), 7868–7881.

Kremheller, A. (2018). The Aerodynamics Development of the New Nissan Qashqai. *SAE Technical Papers*. https://doi.org/10.4271/2014-01-0572.Copyright

Li, X., Yang, T., Liu, J., Qin, X., & Yu, S. (2018). Effects of vehicle gap changes on fuel economy and emission performance of the traffic flow in the ACC strategy. *PLoS ONE*, *13*(7), 1–13.

Luong, T. (2022). *Windshield Distortion Modelling*. Linköping University.

Microsoft. (2024). *Define and solve a problem by using Solver*. Microsoft Support. https://support.microsoft.com/en-us/office/define-and-solve-a-problem-by-using-solver-5d1a388f-079d-43ac-a7eb-f63e45925040

Muthuvel, A., Murthi, M. K., Sachin, N. P., Koshy, V. M., Sakthi, S., & Selvakumar, E. (2013). Aerodynamic Exterior Body Design of Bus. *International Journal of Scientific and Engineering Research*, *4*(7), 2453–2457.

Oh, Y., Park, J., Lee, J., Do, M., & Park, S. (2020). Modeling effects of vehicle specifications on fuel economy based on engine fuel consumption map and vehicle dynamics. *Transportation Research Part D*, *32*, 287–302. https://doi.org/10.1016/j.trd.2014.08.014

Parmar, M. K. (2016). A Technical Review – Comparative Assessment of Aerodynamic Forces Generated Due to Wind Deflector of Passenger Car by CFD and Experimental Method. *International Journal of Engineering Research & Technology (IJERT)*, *4*(10), 1–4.

Pershing, B., & Masaki, M. (1976). *Estimation of Vehicle Aerodynamics Drag*.

Qu, X., & Xie, J. (2021). Simulation Analysis for Effect of Rear Structure of Hatchback Car on Rear Field Characteristics. *Journal of Physics: Conference Series - CCME*. https://doi.org/10.1088/1742-6596/1815/1/012001

Ritme. (2024). *Design-Expert*. https://ritme.com/en/software/design-expert/

Sabiet Ethiopia. (2023). *Anbessa Bus Routes*. Anbessa Bus Routes and Informations.

Solidworks. (2022). *Why Choose SOLIDWORKS 3D CAD?*

Stat-Ease Inc. (2024). *DESIGN EXPERT*. https://www.statease.com/software/design-expert/

Thorat, S., & Rao, G. A. P. (2011). Computational Analysis of Intercity Bus with Improved Aesthetics and Aerodynamic Performance on Indian Roads. *International Journal of Advanced Engineering Technology*, *2*(3).

Vignesh, S., Gangad, V. S., Jishnu, V., Krishna, A., & Mukkamala, Y. S. (2019). Windscreen angle and Hood inclination optimization for drag reduction in cars. *Procedia Manufacturing*, *30*, 685–692. https://doi.org/10.1016/j.promfg.2019.02.062

White, F. M. (2011). *Fluid Mechanics* (Seventh Ed). McGraw Hill.

Wu, J., Posen, I. D., & Maclean, H. L. (2021). Trade-offs between vehicle fuel economy and performance: Evidence from heterogeneous firms in China. *Energy Policy*, *156*. https://doi.org/10.1016/j.enpol.2021.112445

Wu, L. L., Fu, Y., Bu, X. B., Li, X. R., & Ma, X. L. (2020). Research on automatic aerodynamic optimization for a SUV based on RBF model. *Journal of Physics: Conference Series - IWAACE*. https://doi.org/10.1088/1742-6596/1550/4/042025

Yadav, D., Chauhan, S., Karki, S., Nayak, S. ranjan, Kumar, N., & Babu, S. S. (2017). CFD Analysis for Drag Force Reduction in Inter-City Buses. *International Research Journal of Engineering and Technology*, *4*(5), 350–355.

Zhang, Y., Jian, J., Wang, G., Jia, Y., & Zhang, J. (2022). Research on Vehicle Aerodynamics and Thermal Management Based on 1D and 3D Coupling Simulation. *Energies*, *15*, 1–28.

Zhengzhou Yutong Group Co. Ltd. (2019). *ZK6126HGA Series Bus Parts Catalog*.

Zolet, T. L., Rosa, S. C., & Junior, J. S. (2018). On the development of a Fully Automated numerical methodology to improve vehicle ’ s aerodynamics optimizing its external shape. *SAE Technical Paper Series*.

APPENDIX

Appendix 1: Letter Acquired for Data Collection

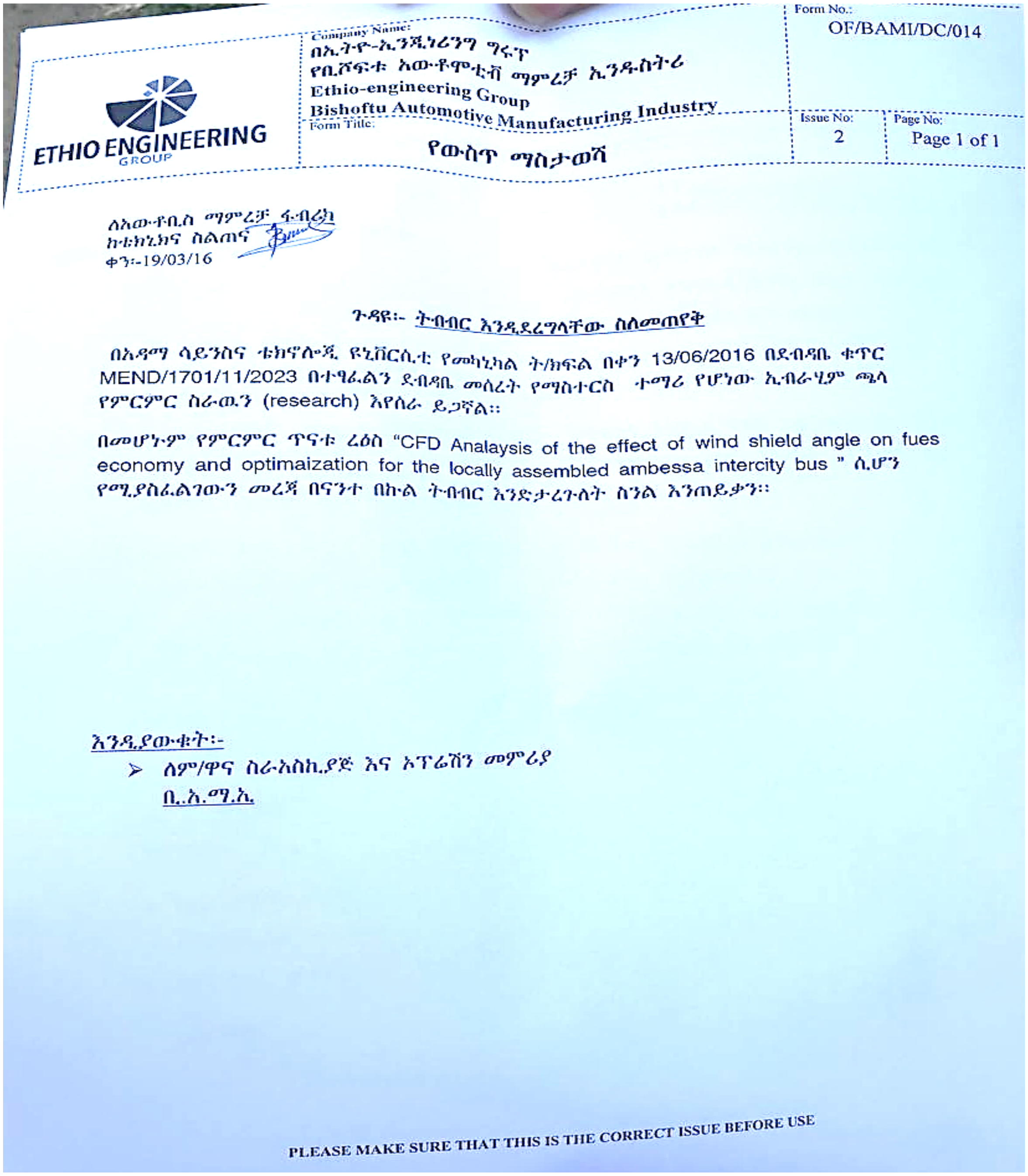

ETHIO ENGINEERING GROUP

Company Name:
በኢትዮ-ኢንጂነሪንግ ግሩፕ
የቢሾፍቱ አውቶሞቲቭ ማምረቻ ኢንዱስትሪ
Ethio-engineering Group
Bishoftu Automotive Manufacturing Industry

Form No.: OF/BAMI/DC/014

Form Title: የውስጥ ማስታወሻ

Issue No: 2

Page No: Page 1 of 1

ለአውቶቢስ ማምረቻ ፋብሪካ
ከቴክኒክና ስልጠና
ቀን፡-19/03/16

ጉዳዩ፡- ትብብር እንዲደረግላቸው ስለመጠየቅ

በአዳማ ሳይንስና ቴክኖሎጂ ዩኒቨርሲቲ የመካኒካል ት/ክፍል በቀን 13/06/2016 በደብዳቤ ቁጥር MEND/1701/11/2023 በተፃፈልን ደብዳቤ መሰረት የማስተርስ ተማሪ የሆነው ኢብራሂም ጫላ የምርምር ስራዉን (research) እየሰራ ይጋኛል።

በመሆኑም የምርምር ጥናቱ ረዕስ "CFD Analaysis of the effect of wind shield angle on fues economy and optimaization for the locally assembled ambessa intercity bus " ሲሆን የሚያስፈልገውን መረጃ በናንተ በኩል ትብብር እንድታረጉለት ስንል እንጠይቃን።

እንዲያውቁት፡-

- ለም/ዋና ስራአስኪያጅ እና ኦፐሬሽን መምሪያ
  በ..አ.ማ.ኢ.

PLEASE MAKE SURE THAT THIS IS THE CORRECT ISSUE BEFORE USE

Appendix 1: Letter acquired from Ethio Engineering group for Data Collection

Appendix 2: Anbessa City Bus Route Start and Destination

Bus Number	Route Start	Route Pass-by	Route Destination	Route Kilometers
1	Megenagna	Gurd Shola	Kara	7.7
2	Kore Mekanisa	Lideta	Addis Ketema	11.1
3	Ayertena	Mexico	Minilik Square	10.8
4	Kaliti	Kira	Merkato	19.4
5	Kore Mekanisa	SARBET	Minilik Square	12.7
6	Kera	MEXICO	Addisu Gebeya	9.9
7	Megenagna	Kotebe	Aleltu	49
8	Kechene	PIYYASA	Merkato	9.4
9	Birass Cilinic Bole School	Kasanchiz	Piazza	10.5
10	Kotebe Teachers Collage	Kebena	Piazza	12.7
11	Kolfe	Atkilt tera	Minilik Hospital	10
12	Gurara	FRENCAY/KILA	Merkato	9.9
13	Italy Embassy	Sinima Ethipia	Merkato	9.9
14	PIYYSA	STADIUM	BULBULA	12.3
15	Megenagna	Abuare	Merkato	10.5
16	Kidanemihret	Afnch Ber	Merkato	7.9
17	kusquam	kidste Mariam	Merkato	9.1
18	keraniyo	kolfe Dildy	Merkato	7.3
19	Asko	Pawlos	Piazza	12.3
20	Dile Ber	RUFAEL	Merkato	8.6
21	Flidoro	kolfe Dildy	Merkato	8.6
22	Summit/codominium/	22 mazoria	Legehar	12.3
23	Lamberet	Afnch Ber	Merkato	12.4
24	Dire Sololia	ASCO	Merkato	15.9
25	Legehar	Gotera	Akaki	19
26	Merkato	Coca Coal	Sebeta	25.5
27	MEXICO	SARBET	GELAN CONDI.	14.9
28	Asko Sansuzi	Mesalemia	Merkato	11.1

Bus Number	Route Start	Route Pass-by	Route Destination	Route Kilometers
29	Addisu Sefer	Teklehaimanot	Merkato	12.7
30	MIZAN AMAN	Semen Gegeya	Merkato	25.5
31	Legehar	4 kilo	Shiromeda	7.4
32	Hana Mariyame Kotebe	22 Mazoria	Legehar	10.6
33	Kotebe Gebiriel	Kebena	4 Kilo	11.4
34	Germen Square	Kera	Merkato	9.8
35	Lebu Musica bet	Lafto	Merkato	15
36	Kara Kore	Torhailoch	Legehar	11.7
37	Keraniyo	Mexico	Mimilik Square	12
38	Lebu Musica Bete	Minilik Square	6 Kilo	11
39	Bole School Medhanialem	Kazanchiz	Merkato	9.6
40	Kara Alo	4 kilo	Merkato	17.9
41	Eyesus Church	4 kilo	Merkato	8.5
42	Megenagna	Bole	Bole Legehare	9.8
43	Megenesha	ASCO	Merkato	30.2
44	Legedadi	4 kilo	Merkato	30.4
45	Legehar	Piazza	Dilbere	8.6
46	Gergi	22 mazoria	4 Kilo	11.2
47	Yenegew Fire School	Mechael	Merkato	6
48	ADDISUGEBEYA	PIYYSA	BOLE	10.9
49	Ayat Condominium	C.M.C	Megenagna	8.8
50	Ayeretena	Torhailoch	Megenagna	12.1
51	Betel Hosipital	Zenbwork	Merkato	10.9
52	Gergi	Bole	Merkato	14.1
53	Bole Michael	Meskel square	Shiromeda	11.5
54	Lafeto	Kera	Leghar	9.5
55	Legehar	4 kilo	Gurara	9.5
56	Saris Abo	Meskel Square	Shiromeda	14.2
57	Kara	22 Mazoria	Leghar	14.4
58	Alem Bank	Torhailoch	Leghar	12
59	Betel Hospital	Coca Cola	Mililik Sqare	11.5
60	Deber Zeit	Gotera	Leghar	47.2

Bus Number	Route Start	Route Pass-by	Route Destination	Route Kilometers
61	Ayat Condominium	22 Mazoria	Leghar Through Kasanchis	15.8
62	Sebeta	Torhailoch	Leghar	23.8
63	Merkato	Atena Tera	Mikililand/Birechko fabrica	9.1
64	6 Kilo	Kazanchiz	Megenagna Gorfe Aswegaj	9.5
65	Merkato	Coca cola	Alem Bank	11
66	Merkato	coca cola	Karakore	10.5
67	Mekanisa Jemo	mexico	Legehar	10.2
68	Torhailoche	Gibi Gebriel	Minlik Hospital	10.2
69	Philpos Church	Mesalemia	Merkato	5.9
70	AJANBO CONDI.	Mexico	PIYASA	11
71	Gerji	Bole Tenatabia	Balcha Hospital	11
72	Hanamariam	58 kebele	Saris Abo	3.8
73	Legehar	Torhailoch	Wingate School	10.2
74	C.M.C Michael	Tikur Anbessa	Merkato	13.3
75	6 Kilo	Kazanchiz	Kera	10.4
76	Megenagna	Zerihun bulding	Kaliti	18.4
77	Ayertena	Sar bet	Kera	13
78	Megenagna	Bherawi	Gofa Condo	12.4
79	4 Kilo	Signal	Summit	12.7
80	Semen Gebeya	Kazanchiz	Megenagna	12.4
81	SANSUSI	PIYYSA	MEGENAGNA	13
82	Sefera Goro	24 kebele	Balcha Hospital	14.6
83	Ayat Condominium	kebena	6 Kilo	18
84	Kolfe	Amanuel	Legehar	9.5
85	Merkato	18 Mazoria	Holeta	45
86	Ayertena	Mebrat Hail	Korki Fabrica	12.3
87	Wingate college	Ketena 2	Ayertena	10.5
88	ADDIS KETEMA	Piazza	Chancho	40
89	ADDIS KETEMA	4 Kilo	Sendafa	44
90	Betel Hospital	Torhailoch	Legehar	10
91	Merkato	Torhailoch	Teji	52

Bus Number	Route Start	Route Pass-by	Route Destination	Route Kilometers
92	Hanamariam	Sar bet	Balcha Hospital	9.6
93	Bole Bulbula	Bole Airport	Megenagna	15.2
94	Piazza	Pawlos	Mekililand Birchko Fabrica	9.9
95	Merkato	Fil Doro	Addisalem	47
96	Megenagna	Anbessa Gerag	Goro Sefera	7
97	Megenagna	Ayat	Legetafo	15.8
98	Dukem	Gelan	Saris Abo	26.3
99	Ayertena	Welete	Alemgena	8.3
100	Jemo Site	Dese Hotel	Merkato	14.5
101	Megenagna	Ayat	Yeka Ayat Con.1sq	12
102	Legehar	Magenagna	Karalo	13.7
103	Jemo 3	Mexico	Piazza	12.2
104	Addisu Gebeya	Mexico	SARIS	12
105	Lagehar	TORHAYLOCHE	Anfo meda	12
106	MEXICO	SARBET	KOYEFECHE	10.8
107	TULUDIMTU	MEXICO	PIYASA	11.4
108	Minilik square	Winget	Asco Addisu Sefer	9.3
109	Saris Abo	Kaliti	tulu dimtu	12
110	Akaki	Meskel Square	6 kilo	24.9
111	Piazza	Medhanialm school	Dire Sololiya	16.6

Appendix 2: Anbessa City Bus Route Start and Destination (Sabiet Ethiopia, 2023)

Appendix 3: The Simplified Model 1 (Current Model) Anbessa Bus

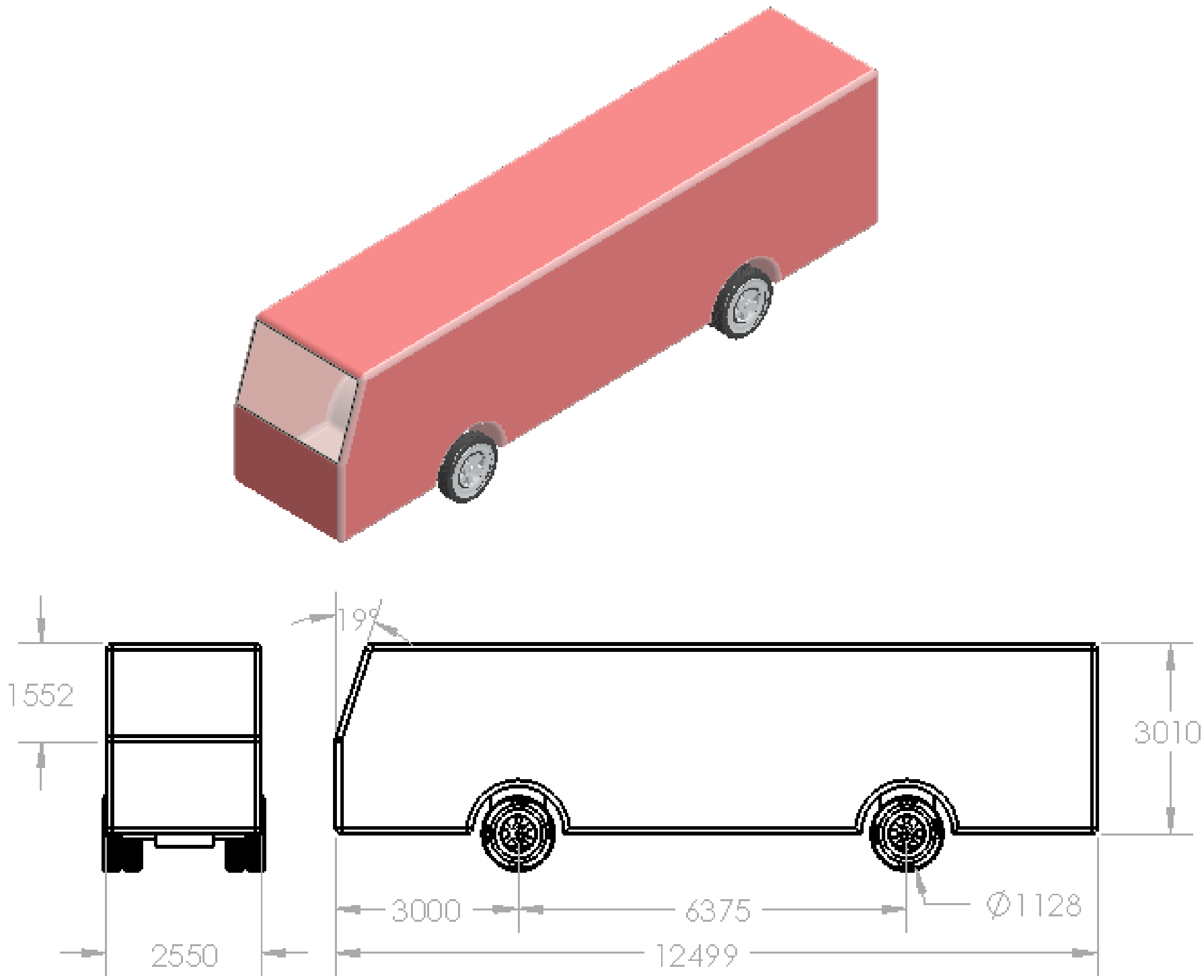

Appendix 3: The simplified model 1 of current Anbessa Bus

Appendix 4: The new model 2 of Anbessa Bus

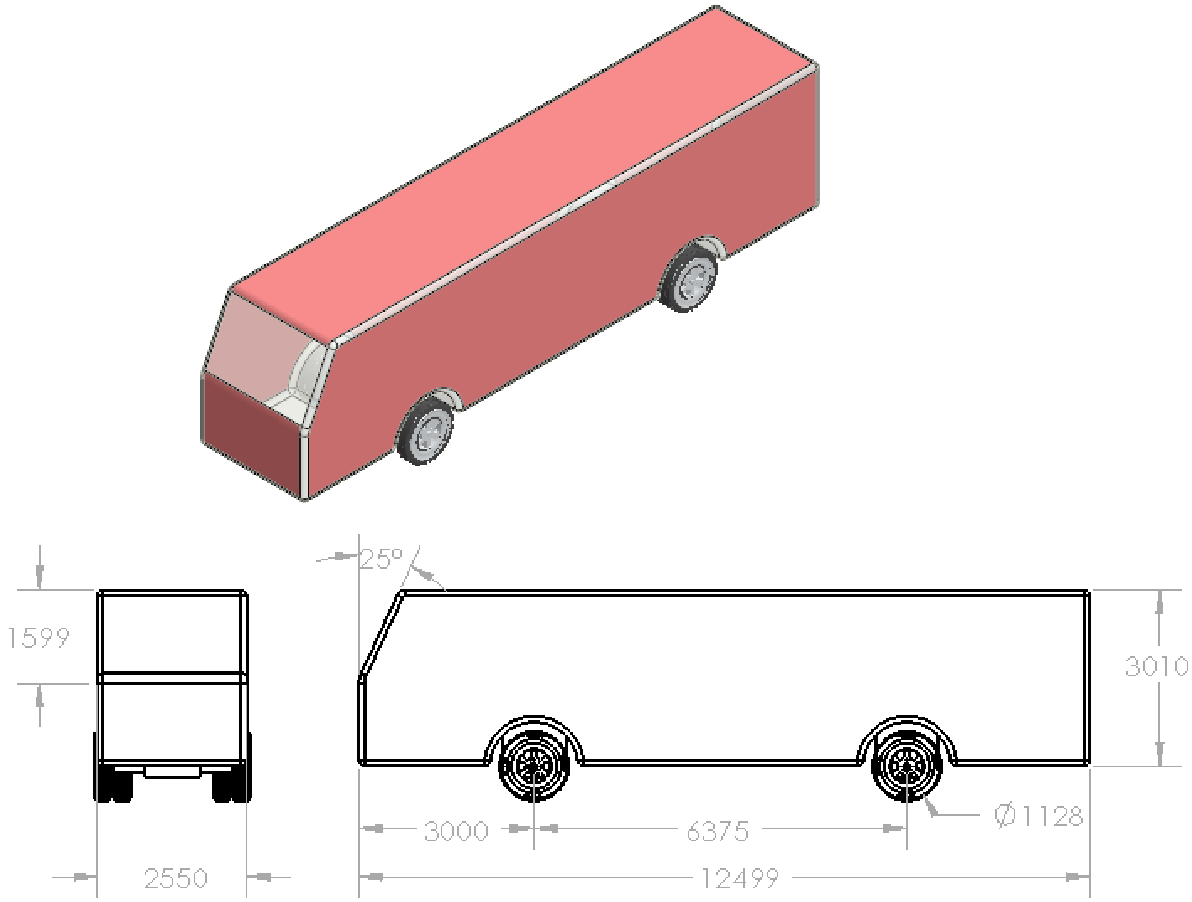

Appendix 4: The new model 2 of Anbessa Bus

Appendix 5: The new model 3 of Anbessa Bus

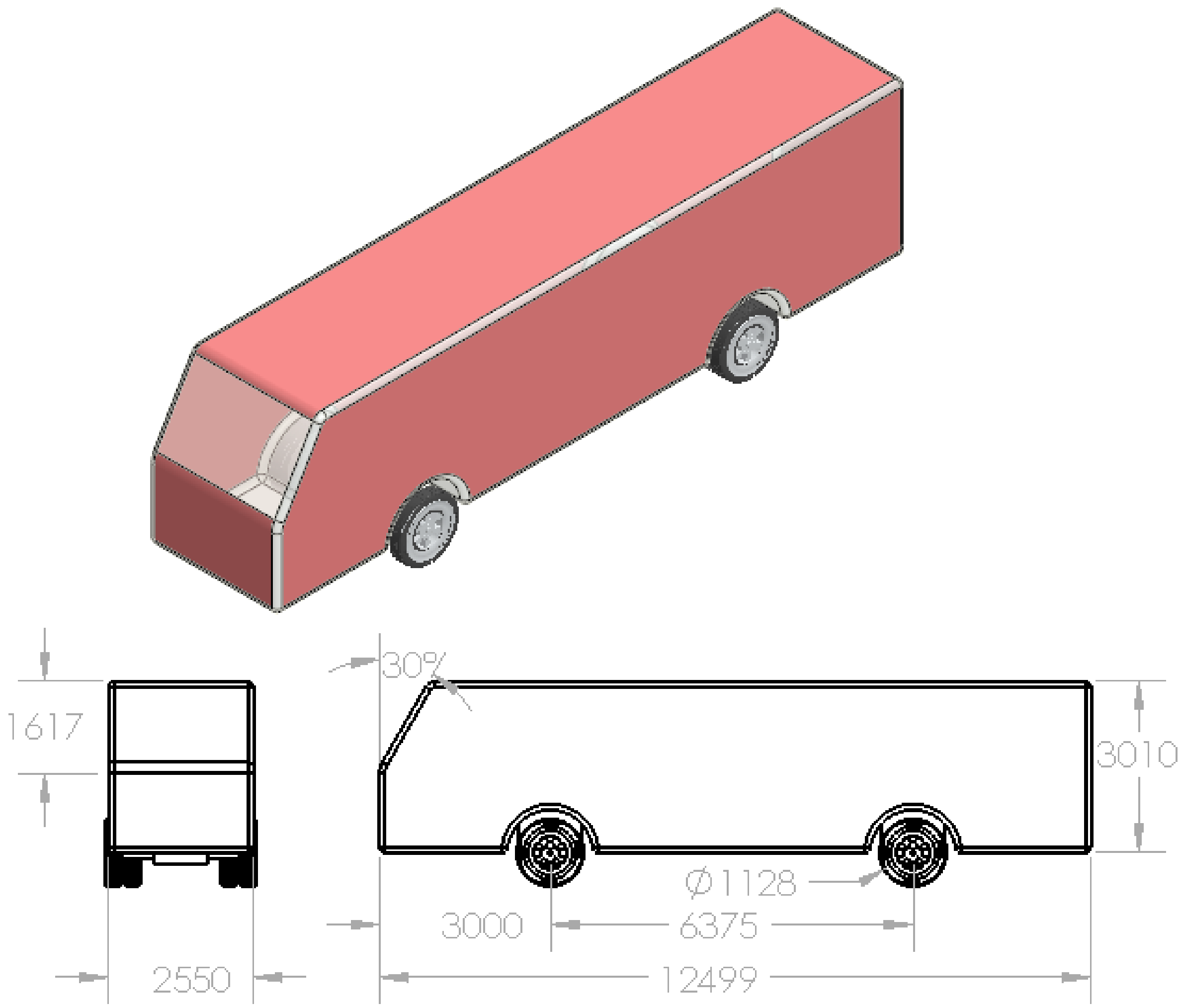

Appendix 5: The new model 3 of Anbessa Bus

Appendix 6: The new model 4 of Anbessa Bus

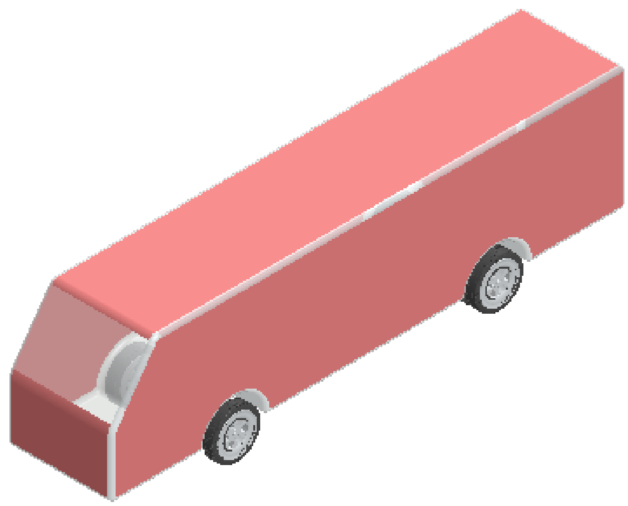

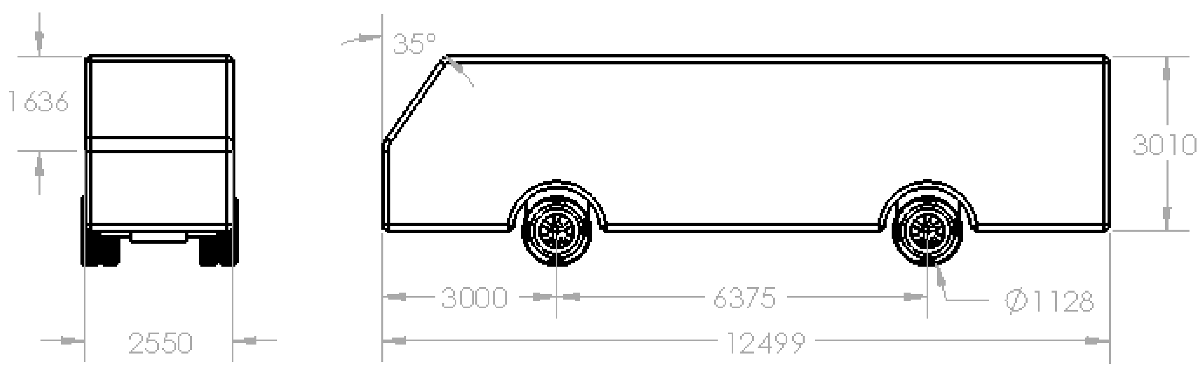

Appendix 6: The new model 4 of Anbessa Bus

Appendix 7: The new model 5 of Anbessa Bus

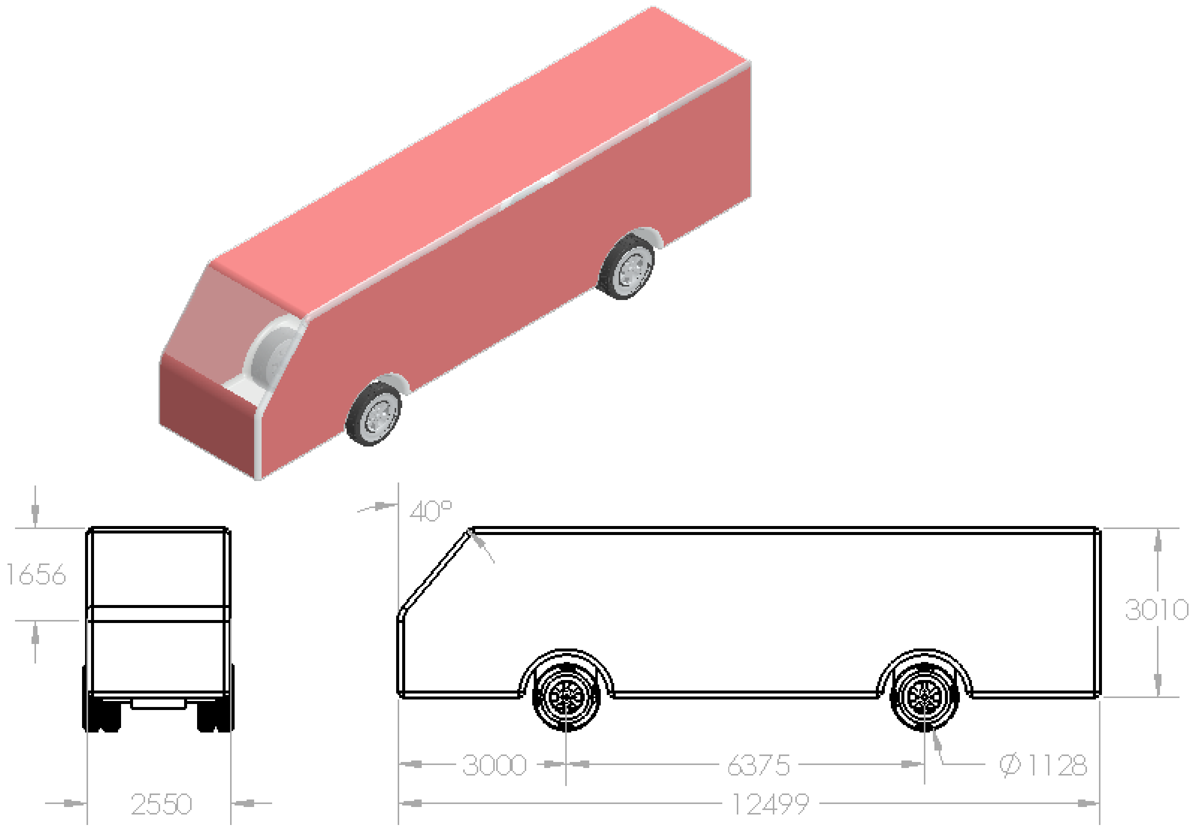

Appendix 7: The new model 5 of Anbessa Bus

Appendix 8: The new model 6 of Anbessa Bus

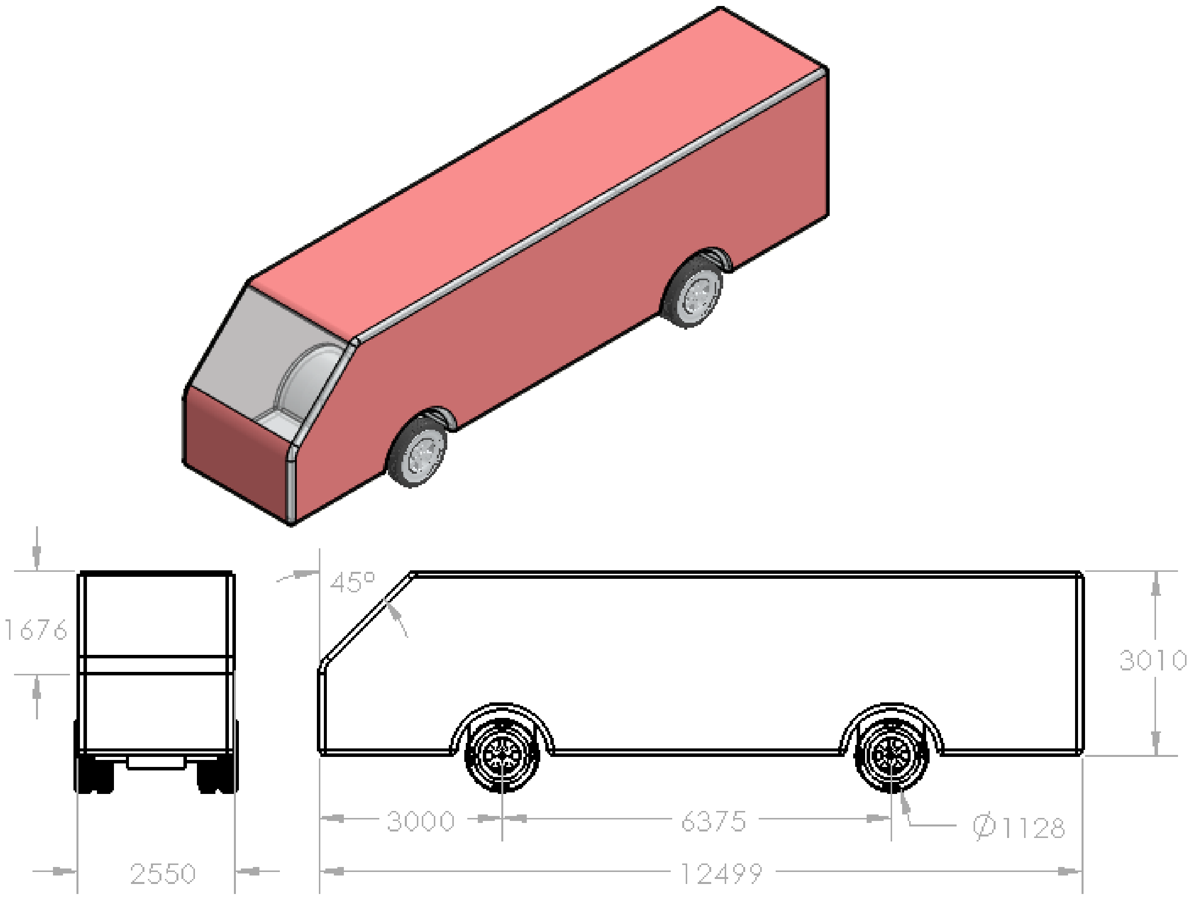

Appendix 8: The new model 6 of Anbessa Bus

Appendix 9: SolidWorks Model of Tire of Anbessa Bus

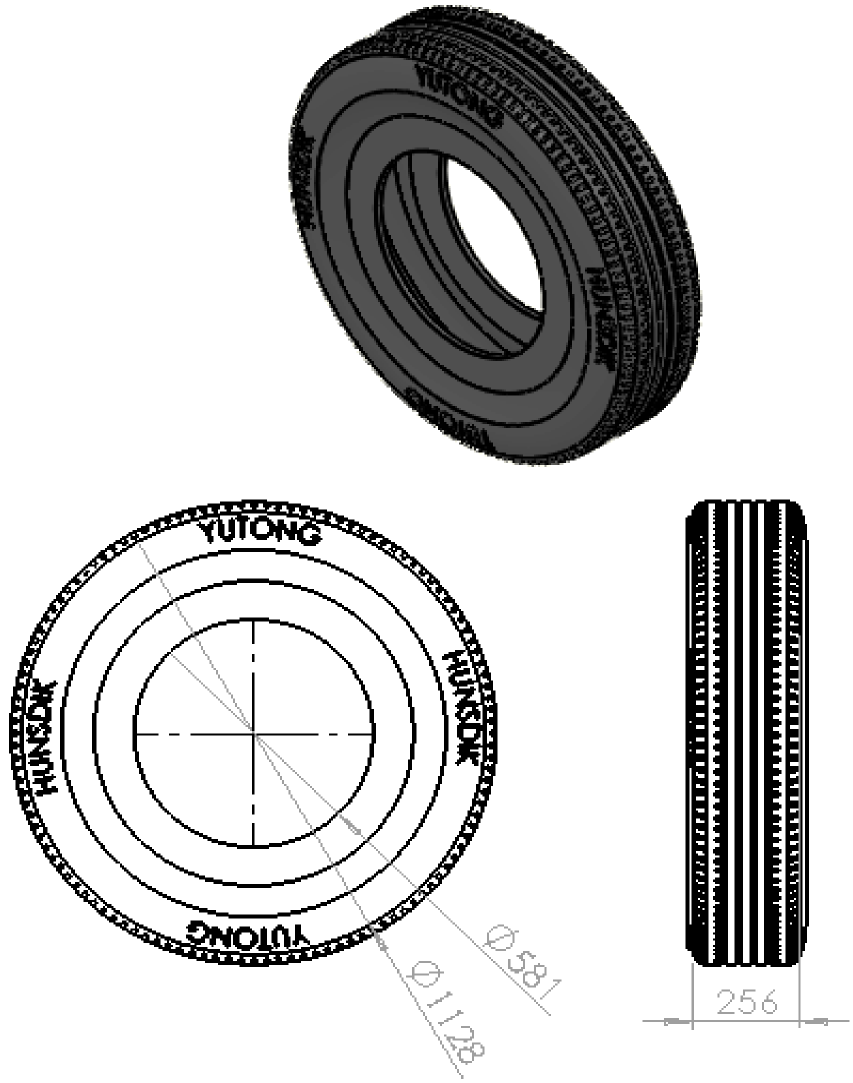

Appendix 9: Tire Model of Anbessa Bus

Appendix 10: SolidWorks Model of Inner Rim of Anbessa Bus

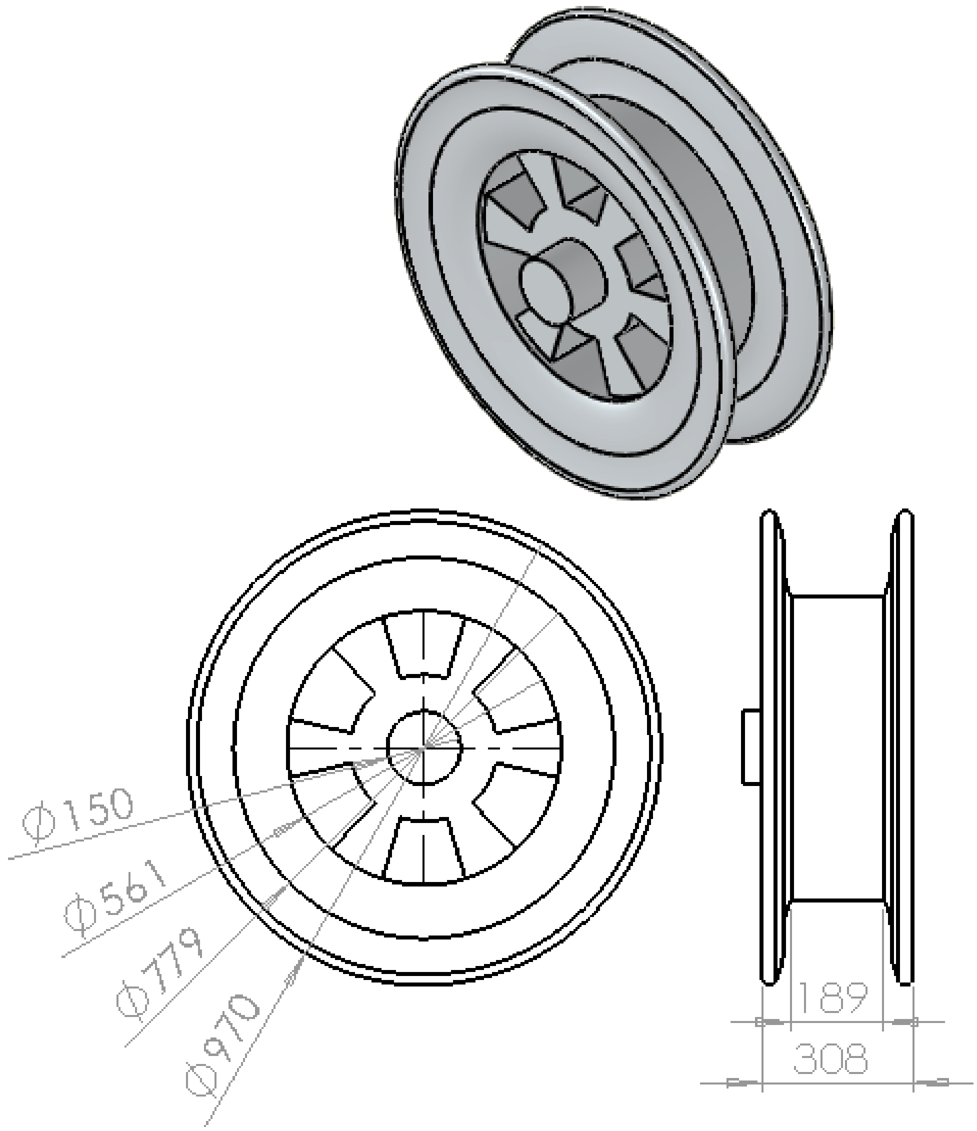

Appendix 10: SolidWorks Model of Inner Rim of Anbessa Bus

Appendix 11: SolidWorks Model of Outer Rim of Anbessa Bus

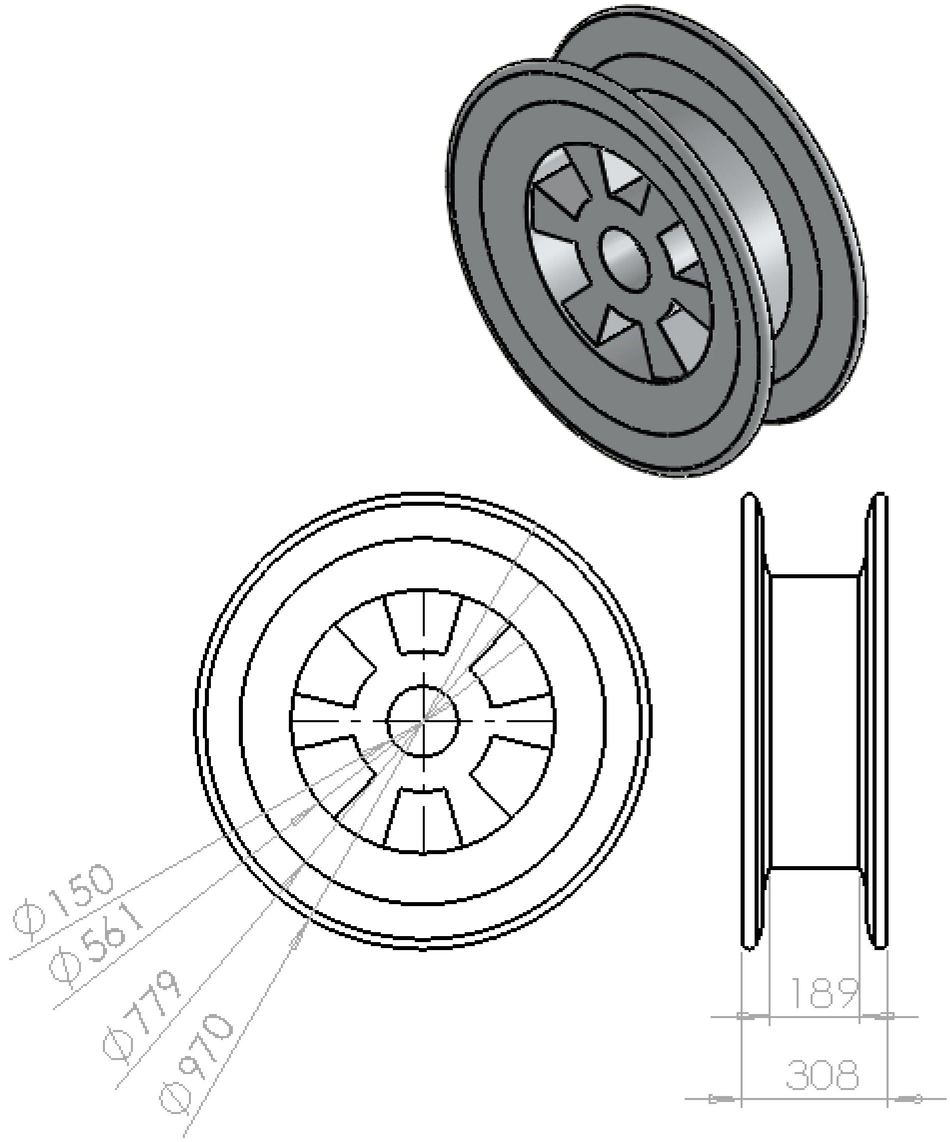

Appendix 11: SolidWorks Model of Outer Rim of Anbessa Bus

Appendix 12: SolidWorks Model of Front Wheel of Anbessa Bus

Appendix 12: SolidWorks Model of Front Wheel of Anbessa Bus

Appendix 13: SolidWorks Model of Rear Wheel of Anbessa Bus

Appendix 13: SolidWorks Model of Rear Wheel of Anbessa Bus